Electronic Supplementary Material (ESI) for Materials Advances.

Supplementary Information:

White light emission generated by two stacking patterns of a single organic molecular crystal

Yuma Nakagawa,*[a] Kuon Kinoshita,[a] Megumi Kasuno,[a] Ryo Nishimura,[b] Masakazu Morimoto,[b] Satoshi Yokojima,*[c,d] Makoto Hatakeyama,[d,e] Yuki Sakamoto,[d] Shinichiro Nakamura[d] and Kingo Uchida*[a,d]

[a] Department of Materials Chemistry, Faculty of Science and Technology, Ryukoku University, Seta, Otsu, Shiga 520-2194, Japan.

[b] Department of Chemistry and Research Center for Smart Molecules, Rikkyo University, 3-34-1 Nishi-Ikebukuro, Toshima-ku, Tokyo 171-8501, Japan.

[c] School of Pharmacy, Tokyo University of Pharmacy and Life Sciences, 1432-1 Horinouchi, Hachioji, Tokyo 192-0392, Japan.

[d] RIKEN, Cluster for Science, Technology and Innovation Hub, Nakamura Laboratory, 2-1 Hirosawa, Wako, Saitama 351-0198, Japan.

[e] Faculty of Pharmaceutical Science, Sanyo-Onoda City University, 1-1-1 Daigakudori, Sanyo-Onoda, Yamaguchi 756-0884, Japan.

Table and Contents

Materials and Methods

1. General information

^{1}H (400 MHz), ^{13}C (100 MHz), and ^{19}F NMR (376 MHz) spectra were recorded at room temperature with a JEOL JNM-400 spectrometer. Chemical shifts of ^{1}H and ^{13}C NMR are given in parts per million (ppm) using the residual solvent peak(s) as a reference.[S1] Chemical shifts of ^{19}F NMR are given in ppm using C_6F_6 (-164.9 ppm). Multiplicities of the signals are described as follows: s = singlet, m = multiplet or overlap of nonequivalent resonances. The NMR spectra of compounds were recorded in $CDCl_3$. Melting points were measured on Yanaco MP-500D. The apparent pH of the organic solvent was measured with a HORIBA pH METER D-52. The high-resolution mass spectrometry (HRMS) was recorded with a JEOL JMS-S3000 SpiralTOF. Absorption spectra of the solutions were monitored with a Hitachi U-4150 spectrophotometer. Fluorescence spectra of the solutions and excitation spectra of the crystals were monitored with a Hitachi F-7100 Fluorescence Spectrophotometer equipped with Toshiba colour filters (UV-35). Fluorescence spectra in **1ar** solution were measured by adjusting the absorbance at the excitation wavelength to 0.05 ± 0.005, unless otherwise noted. Fluorescence quantum yields of the solutions were calculated from the relative ratio using 9,10-diphenylanthracene in ethanol (Φ_{Flu} = 0.96)[S2]. Fluorescence spectra, absorption spectra, and absolute fluorescence quantum yields of the crystals were monitored with a Hamamatsu photonics Quantaurus-QY. Fluorescence lifetime measurements were monitored with a Hamamatsu photonics Quantaurus-Tau. Excitation spectra of the crystals were monitored with a Hitachi F-7100 Fluorescence Spectrophotometer. Optical microscopic images were recorded with a KEYENCE VH-S30. For the UV light irradiation, a UV hand lamp SPECTROLINE Model EB-280C/J (λ = 313 nm), an AS ONE Handy UV Lamp LUV-6 (λ = 365 nm, 810 μW cm^{-2}), and a KEYENCE UV-400, UV-50H (λ = 365 nm, 277 or 544 mW cm^{-2}) were used. All measurements were performed at room temperature unless otherwise specified. Elemental analysis of the compounds was carried out at the Graduate School and Faculty of Pharmaceutical Sciences, Kyoto University. HRMS measurements of the compounds were carried out at the Division of Materials Science, Nara Institute of Science and Technology. The diagram of CIE1931 coordinates was created using ColorAC.[S3]

The Gaussian16 program package[S4] was used for geometry optimization with density functional theory (DFT)[S5,S6] for ground states. The B3LYP[S7-S9] functional was adopted as the exchange-correlation term of DFT. The 6-31G(d,p) basis set was adopted for all calculations. The D2 version of Grimme's dispersion[S10] as an empirical dispersion force model was used for all calculations except for monomer and dimer. Jmol software was used to visualize the Frontier molecular orbitals.[S11] In addition, monomer and dimer calculations were performed by the CIS(D) method.[S12,S13] To better understand the characteristics of each state, we further performed geometry optimization for a monomer by imposing C2v symmetry by B3LYP with a 6-31G(d) basis set. The optimized structure was used to calculate the excited states by TDDFT with B3LYP, CIS(D), and SAC-CI with level1. The 6-31G(d) basis set was used for these calculations.

2. X-ray crystallographic analysis

X-ray crystallographic analysis for **1ar** crystal was performed with an X-ray diffractometer (Bruker AXS, D8 QUEST) with Mo Kα radiation (λ = 0.71073 Å). The crystal was cooled using a low-temperature controller (Japan Thermal Engineering, JAN 2-12). The diffraction frames were integrated with the Bruker SAINT program. The cell constants were determined by global refinement. The data were corrected for absorption effects using the multi-scan method (SADABS). The structure was solved by the direct method and refined by the full-matrix least-squares method using the SHELX-2014 program. The positions of all hydrogen atoms were calculated geometrically and refined by the riding model. The crystallographic data can be obtained free of charge from the Cambridge Crystallographic Data Centre via www.ccdc.cam.ac.uk/data_request/cif (CCDC No. 2159901).

3. Theoretical investigation of the origin of two fluorescent peaks by quantum chemical calculations

3.1 Origin of the broad fluorescent spectrum with two peaks

DFT calculations of **1ar** were performed to gain insight into the optical features in solution (dispersed state) and crystalline state (aggregated state). Full optimization of the structure of each conformer of **1ar** was obtained from X-ray crystallographic analysis for the ground state at the B3LYP/6-31G(d,p) level of theory. Calculation of vibrational frequencies is carried out to confirm that the optimized structure corresponds to a minimum on the potential energy surface. Then, the first 15 singlet excited states were calculated by the time-dependent (TD)[S14-S16] DFT method based on the B3LYP/6-31G(d,p) level of theory. The excited state calculations were performed (1) for the optimized structure of **1ar** (2) for the structures extracted from X-ray crystallographic analysis data for monomers, a unit cell consisting of tetramer, and 8-9mers, and (3) for the structures where the molecular packings were the same as (2) but with each conformer replaced with an optimized structure.

The lowest excitation energies of monomer of **1ar** calculated by TDDFT in Table S7† agrees with the energetically lowest peak in the experimental absorption spectrum in Fig. S5†. In comparison with the results in Table S4†, where the X-ray crystallographic structure was employed instead of the geometry optimized structure in Table S7†, we found that the excitation energy is reduced by about 0.1 eV. We can expect a similar energy reduction for the aggregated case by replacing each monomer in the crystal by the optimized structure. Thus, we further calculated the excitation energies for aggregates of **1ar** assembled as in the crystal structure.

The lowest excitation energy of molecules of **1ar** in a unit cell was slightly reduced in comparison with those of the monomers. The excitation energies from the first to 4th excited states have similar values due to the fact that those states are approximately linear combinations of the lowest excited state of four monomers in the unit cell. The oscillator strength of the lowest excited state is nearly zero, whereas two states with large oscillator strength exist only at slightly higher energies (2nd and 4th excited states). We discuss this point later. The shift of the wavelength from the monomer to the

tetramer in the unit cell is small due to the fact that the four molecules are spatially apart. Thus, we further calculated larger systems to include the effects of π-stacking and neighbouring molecules.

As shown in Tables S5 and S6†, the lowest excitation energies are further reduced by increasing the size. By replacing each monomer with the optimized structure, the lowest excitation energy become 3.11 eV (399.21 nm) for the large supercell extended by 0.5 unit cells for the *a* and *b* axes. A large shift of the absorption edge is due to the spatially spreading excited state consisting of a π-orbital over many molecules. Thus, for a much larger size, as in the crystal of **1ar** together with the relaxation of the structure, the large shift of the second peak (565 nm) in Fig. 2(h) may be one explanation.

As for the first peak in the fluorescence spectrum around 425 nm, we assume that it is mainly due to the decay from the localized state in monomer. If the excited state (energy) migrated to lower energies states, we would not be able to observe the short lifetime in Fig. 2 (i). This short lifetime in Fig. 2 (i) suggests that the excited state is localized on the monomer, and it is relaxed quickly enough.

3.2 Origin of the strong fluorescence

Here, we noticed that all of the oscillator strength of the lowest excited states in these calculations, except monomer, are zero or very small. In experiment, by contrast, we observed a strong fluorescence. In order to understand this point, we further performed the excited state calculations by different methods.

We first performed CIS(D) calculations for dimers of **1ar**. The CIS(D) calculation estimates the excitation energies of excited states by perturbatively including the effect of the double excitation on the CIS energies. As shown in Fig. 4b, there are four types of stacking dimer. For convenience, we call these dimers Type 1 to Type 4 from left to right in Fig. 4b. Type 1 and Type 2 are dimer of conformer A, and others are dimer of conformer B. Although there are subtle differences in the excited states of these dimers, overall, the results are similar (Tables S10 and S11†). As in Table S11†, the excited states obtained by CIS resembles those of TDDFT in Table S10†, except that the excitation energies are over-estimated. In contrast, the excitation energy of the 4^{th} excited state in CIS become the lowest excited state in CIS(D). Since this state has a large oscillator strength, this result is consistent with the experimental result. This suggests that the inclusion of double excitation is critical.

To confirm this result, we performed monomer calculations (Tables S12 and S13†). First, to check that the main character of excited states does not change by imposing the C2v symmetry, CIS(D)/3-31G calculations were performed for both X-ray crystallographic structures and the C2v symmetric structure of monomer of **1ar**. Although there were slight changes in the excitation energies, the lowest three states were quite similar. (Note, for the comparison between three methods in Table S13†, the order of the excited states in CIS and CIS(D) of Table S13† is based on the CIS(D) energy, unlike in Table S12†. Thus, for the comparison between Tables S12† and S13, we need to keep in mind that the first and second excited states in Table S12† correspond to the second and first excited states in Table S13†, respectively.) Among the excited states in C2v symmetric structure, the symmetry of the lowest excited states of TDDFT and CIS is B2, but that of SAC-CI and CIS(D) is A1. The first excited state of TDDFT is due to the HOMO-LUMO transition as in Fig. S13†; the transition dipole moment is in

the horizontal direction. On the other hand, the first excited state of SAC-CI is due to the HOMO-1-LUMO transition as shown in Fig. S14†; the transition dipole moment is thus in the vertical direction. (The MOs of monomers in Figs. S13 and S14† are given by the calculation of X-ray crystallographic structure, but the structure with C2v symmetry produced quite similar results.) By including the effect of double excitations consistently, the lowest excited states by SAC-CI and CIS(D) are A1 symmetric. The TDDFT includes the effect of correlation only partially and consequently gave the wrong order of the first and second excited states.

As for the dimer case, its excited states are given by linear combination of the excited state of two monomers. Thus, both the HOMO and HOMO-1 in Fig. S15† are basically the HOMO of monomer in Fig. S14† but with a different sign for one of the monomers. Similarly, the LUMO and LUMO-1 in Fig. S15† are assigned to the LUMO in Fig. S14† but with a different sign. Other MOs have similar characteristics. The major contributions for the first and second excited states obtained by CIS in Table S11† are due to HOMO→LUMO, HOMO-1→LUMO+1 and HOMO→LUMO+1, HOMO-1→LUMO transitions. Thus, the excitations are attributed to the combination of the HOMO→LUMO transition of monomer with a different phase. In contrast, the major contributions for the third and fourth excited states obtained by CIS in Table S11† are due to HOMO-2→LUMO, HOMO-3→LUMO+1 and HOMO-2→LUMO+1, HOMO-3→LUMO transitions. Thus, the excitations are attributed to the combination of the HOMO-1→LUMO transition of monomer with a different phase. For the dimer case, inclusion of the effect of double excitation by CIS(D) changes the order of the excited states from the fourth to the first, from the third to the second, from the first to the third, and from the second to the fourth.

The change in the order of the third and fourth excited states in CIS become lower energies in CIS(D) due to the change in the order of the excited state of monomer. The change in the order between the third and fourth excited states in CIS due to the inclusion of the effect of double excitation is most likely due to the relative position of the dimer. The structures of these dimers are considered intermediate between J-type and H-type aggregations.[S17,S18] Without inclusion of the effect of double excitations, the excitation is dominant near the π-stacking area, which has the characteristic of H-type aggregation. By the inclusion of the effect of double excitations, it is expected that the excitation would spread and thus produce characteristics of a J-type aggregation.

As for the larger systems, by the inclusion of the effect of double excitations, we thus expect that the lowest excited state would have large oscillator strength by a similar mechanism as that discussed above.

4. Synthesis

Synthesis of 1,2-bis(2-phenylthiazol-4-yl)perfluorocyclopentene (1o)

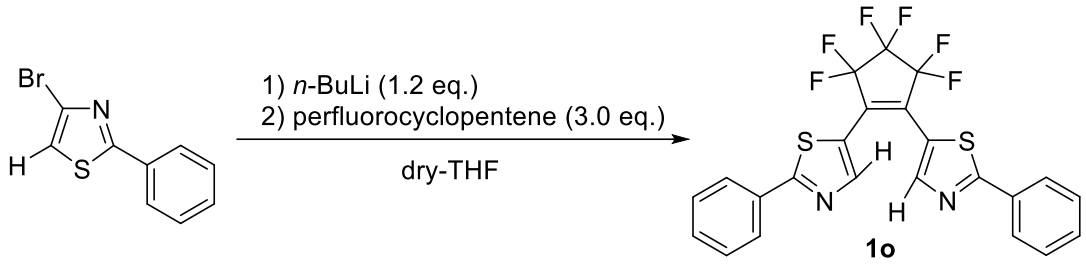

To a 100-mL three-neck flask containing 1.50 g (6.25 mmol) of 4-bromo-2-phenylthiazole, 30 mL of THF anhydrous was added in a dry-ice methanol bath at -78°C in an argon gas atmosphere. To this solution, 4.7 mL (7.50 mmol, 1.2 eq.) of 1.6 N *n*-BuLi hexane solution was gradually added while maintaining the temperature and stirring for 1 h. Then 1.6 mL (18.75 mmol, 3.0 eq.) of perfluorocyclopentene was added, followed by stirring another 30 min, and then the temperature of the reaction mixture was allowed to warm to -50°C. Then the mixture was stirred for 5 h at that temperature. After the reaction was completed, 50 mL of water was added, and the mixture was allowed to warm to room temperature. The solvent of THF was evaporated with a rotary evaporator. The mixture was extracted with 60 mL of diethyl ether applied four times. The organic layer was washed with 100 mL of brine and dehydrated over sodium sulphate anhydrous. After removal of sodium sulphate by filtration, the solvents were removed with a rotary evaporator. Then the obtained residue was purified by silica gel column chromatography, using a mixture of *n*-hexane and ethyl acetate (98: 2 (v/v)) as eluent, to obtain 200 mg (0.404 mmol) of **1o** as pale-yellow crystals in 13% yield.

1o: m.p. 164.4−165.3°C. ^{1}H NMR (400 MHz, $CDCl_3$, ppm) δ 8.20 (s, 2H), 7.98-7.95 (m, 4H), 7.50-7.44 (m, 6H). ^{13}C NMR (100 MHz, $CDCl_3$, ppm) δ 173.0, 147.9, 132.6, 131.6, 129.4, 127.2, 122.3. ^{19}F NMR (376 MHz, $CDCl_3$, ppm) δ -112.7 (s, 4F), -133.7 (s, 2F). HRMS (MALDI, positive): *m/z* calcd. for $C_{23}H_{13}N_2F_6S_2$ $[M+H]^+$: 495.04243, found: 495.04164. Anal. Calcd. for $C_{23}H_{12}N_2F_6S_2$: C, 55.87; H, 2.45; N, 5.67. Found: C, 55.83; H, 2.30; N, 5.66.

Fabrication of 1ar

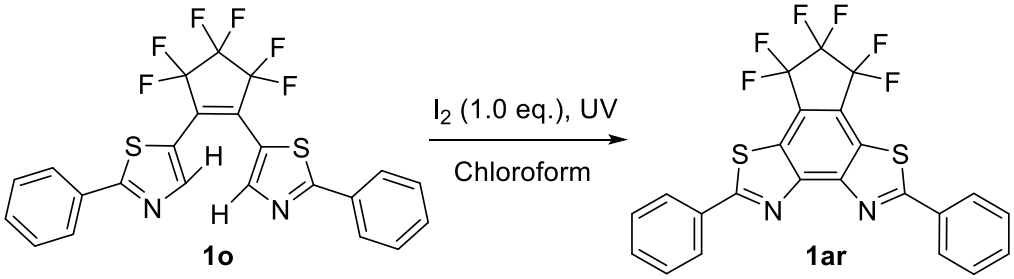

Chloroform (18 mL) containing 45.0 mg (91.01 μmol) of **1o** and 23.1 mg (91.01 μmol) of iodine (I_2) was prepared. The solution was irradiated with UV light (λ = 365 nm, 810 μW cm^{-2}) for 21 h. Then, 2 mL of sat. $NaHCO_3$ aq. and 4 mL of sodium thiosulfate aq. were added to the solution. The solution was extracted with 30 mL of dichloromethane (DCM) three times and dehydrated over sodium sulphate

anhydrous. After removal of sodium sulphate by filtration, the solvents were removed with a rotary evaporator. Then the obtained residue was purified by silica gel column chromatography using a mixture of *n*-hexane and ethyl acetate (96: 4 (v/v)) as eluent to obtain 37.3 mg (75.74 μmol) of **1ar** as white crystals in 83% yield.

1ar: m.p. 265.6-266.3°C. ^{1}H NMR (400 MHz, $CDCl_3$, ppm) δ 8.34-8.31 (m, 4H), 7.63-7.56 (m, 6H). ^{13}C NMR (100 MHz, $CDCl_3$, ppm) δ 173.9, 152.3, 132.5, 132.5, 129.4, 128.5, 115.5. ^{19}F NMR (376 MHz, $CDCl_3$, ppm) δ -111.2 (s, 4F), -132.3 (s, 2F). HRMS (MALDI, positive): *m/z* calcd. for $C_{23}H_{10}N_2F_6S_2Na$ $[M+Na]^+$: 515.00873, found: 515.00778. Anal. Calcd. for $C_{23}H_{10}N_2F_6S_2$: C, 56.10; H, 2.05; N, 5.69. Found: C, 55.94; H, 2.12; N, 5.59.

5. Preparation of 1ar/PS composite films

To prepare the films, 100 mg of polystyrene (PS: $(C_8H_8)_n$, n = 1600-1800) was added to 30 mL of chloroform, and the mixture was heated to dissolve PS. After that, 3 mL of the solution was taken, and **1ar** at 0.01 (0.1 wt%), 1.1 (10 wt%), 2.5 (20 wt%), 4.3 (30 wt%), 6.6 (40 wt%), or 10 mg (50 wt%) dissolved in 1 mL of chloroform was added to it and stirred for 5 min. Finally, the mixture was drop-cast onto a clean glass slide, left at room temperature for 2 h, and then dried in an oven (100°C) for 2 h.

The PS film was prepared under the same conditions as the **1ar**/PS composite film without the addition of **1ar**.

Figures and Tables

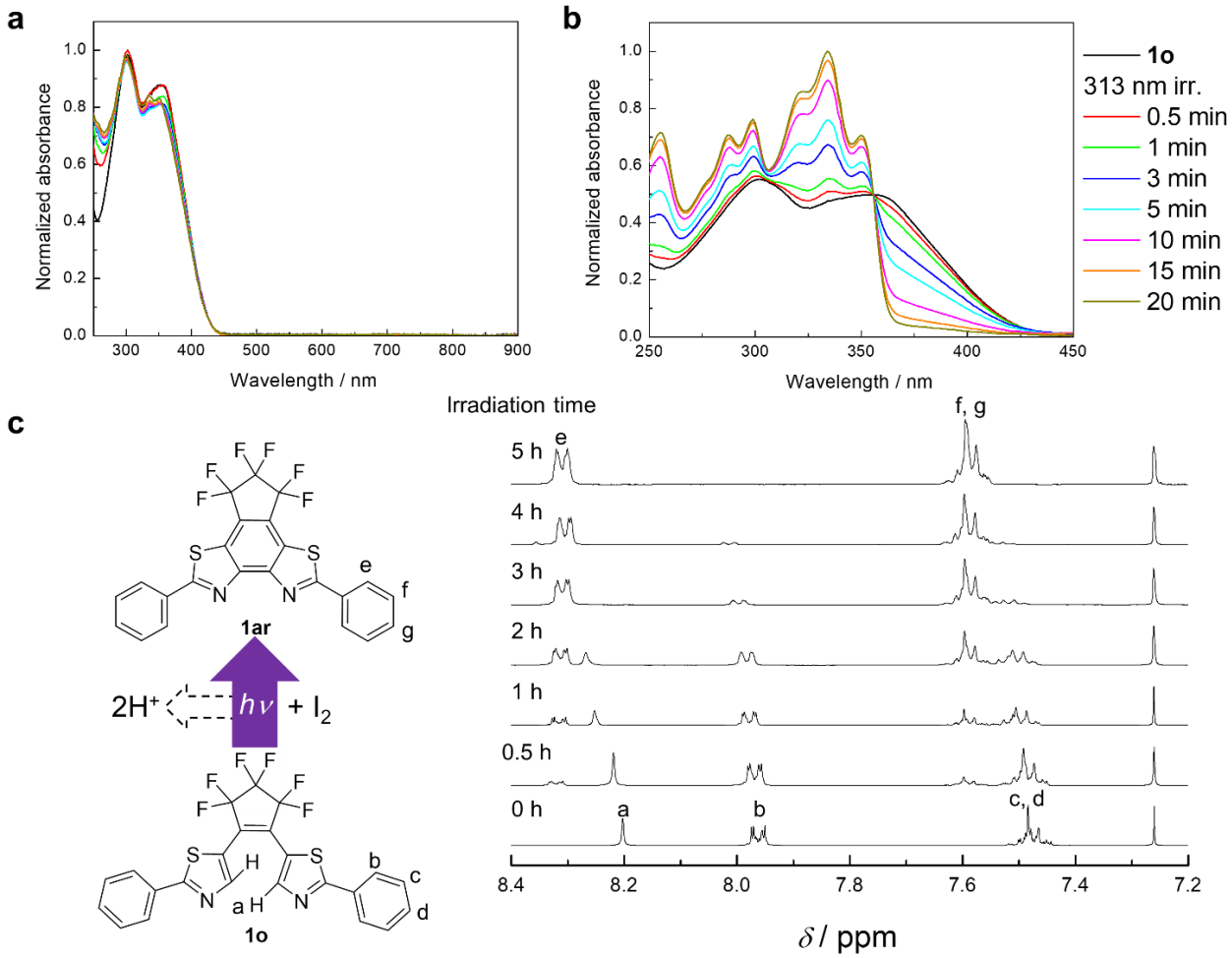

Fig. S1 (a, b) Normalized absorption spectral changes of **1o** irradiated with UV light (λ = 313 nm) in *n*-hexane. Measurements were carried out in the absence (a) and presence (b) of I_2 (**1o**: 15 μM, I_2: 0.01 M). The absorption band is blue-shifted due to the cleavage of the conjugated length in the molecule as the reaction of the fused ring proceeds. (c) ^{1}H NMR spectral changes of **1o** irradiated with UV light (λ = 365 nm, 277 mW cm^{-2}) in the presence of I_2 (**1o**: 3 mg + I_2: 3.1 mg in $CDCl_3$: 0.53 mL). These measurements were performed at room temperature.

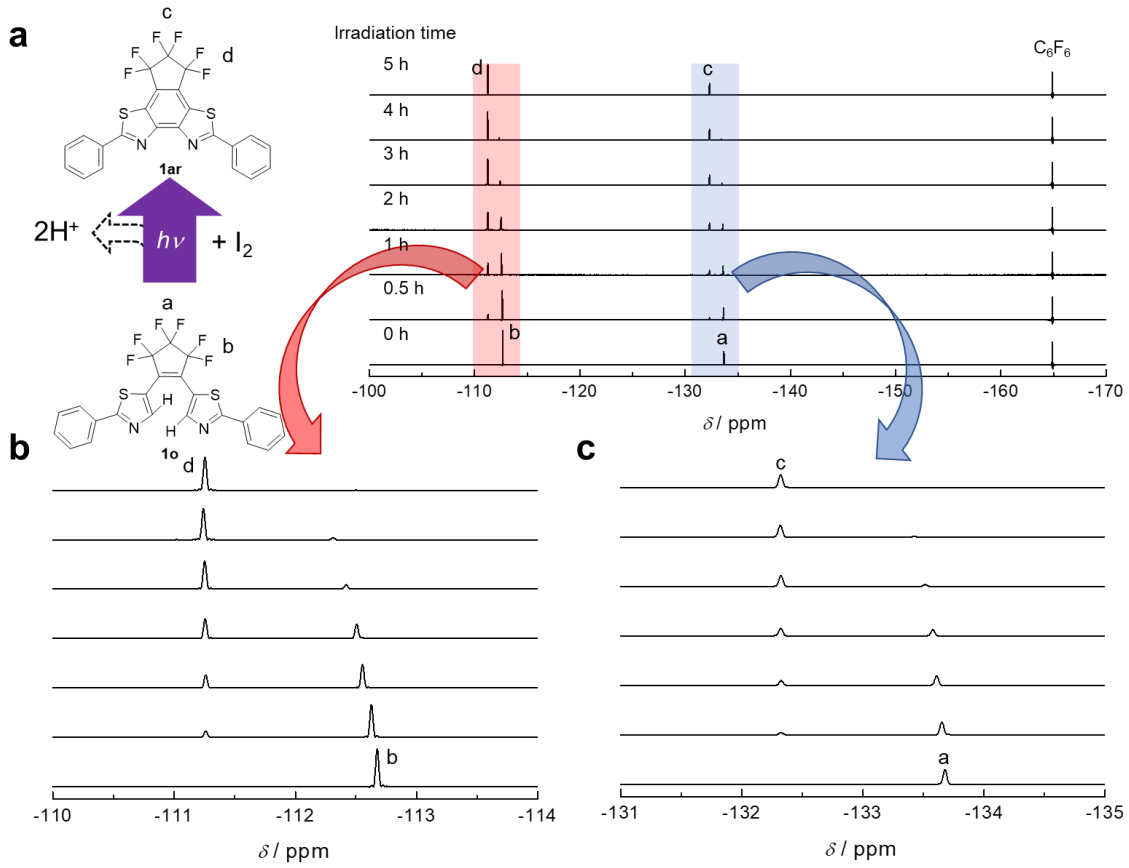

Fig. S2 ^{19}F NMR spectral changes of **1o** irradiated with UV light (λ = 365 nm, 277 mW cm^{-2}) in the presence of I_2 (**1o**: 3 mg + I_2: 3.1 mg in $CDCl_3$: 0.53 mL). These measurements were performed at room temperature.

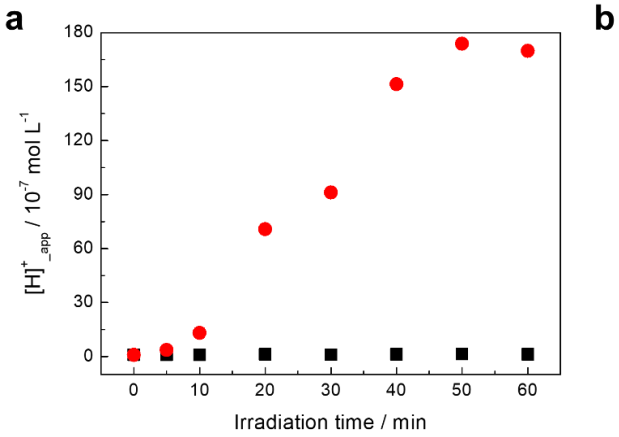

b

Irradiation time / min	pH_app —	pH_app 1o
0	7.01	7.03
5	6.97	6.44
10	6.97	5.88
20	6.90	5.15
30	6.93	5.04
40	6.91	4.82
50	6.88	4.76
60	6.90	4.77

Fig. S3 (a) Plots of apparent hydrogen-ion concentration ($[H]^+_{app}$) vs. UV light (λ = 365 nm, 810 μW cm^{-2}) irradiation in the presence (red circle) or absence (black square) of **1o** in ethanol. (**1o**: 5×10^{-4} M, tetrabutylammonium perchlorate (TBAP): 0.01 M). (b) Change in apparent pH (pH_{app}) due to UV light irradiation in the presence or absence of **1o** measured using a pH meter. The apparent concentrations $[H]^+_{app}$ were determined from the pH_{app} obtained from the measurements. These measurements were performed at room temperature.

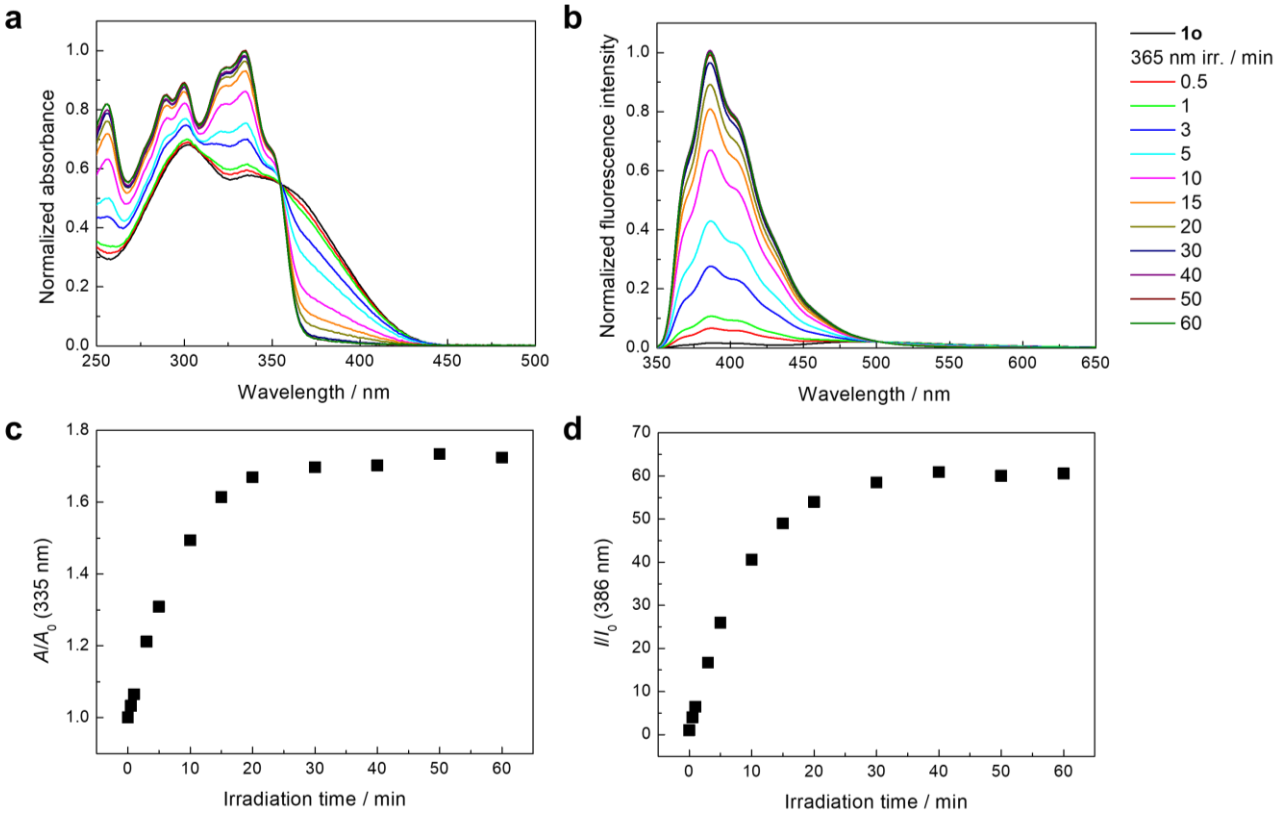

Fig. S4 (a, b) Normalized absorption (a) and fluorescence (b) spectral changes of **1o** by UV light (λ = 365 nm, 810 μW cm^{-2}) irradiation in ethanol in the presence of TBAP (**1o**: 15 μM, TBAP: 0.01 M). The absorption band is blue-shifted due to the cleavage of the conjugated length in the molecule as the reaction of the fused ring proceeds. (c) Plots of A/A_0 vs. UV light irradiation time of **1** at 335 nm in the presence of TBAP. Here, A_0 is the absorption intensity of **1o** at 335 nm before UV light irradiation, and A is the absorption intensity of **1** at 335 nm for each irradiation time. (d) Plots of I/I_0 vs. UV light irradiation time of **1** at 386 nm in the presence of TBAP. Here I_0 is the fluorescence intensity of **1o** at 386 nm in the presence of TBAP without UV light irradiation, and I is the fluorescence intensity of **1** at 386 nm in the presence of TBAP for each irradiation time. As the ratio of **1ar** produced by irradiating **1o** with UV light increased, the fluorescence intensity increased. These measurements were performed at room temperature.

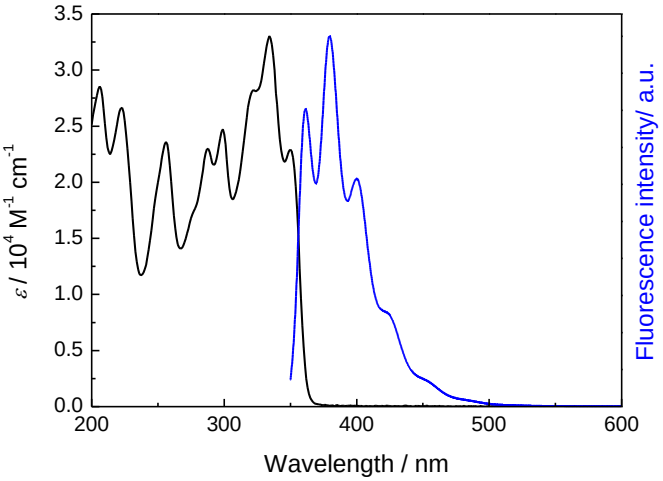

Fig. S5 Absorption and fluorescence spectra of **1ar** in *n*-hexane (λ_{exc} = 336 nm). These measurements were performed at room temperature.

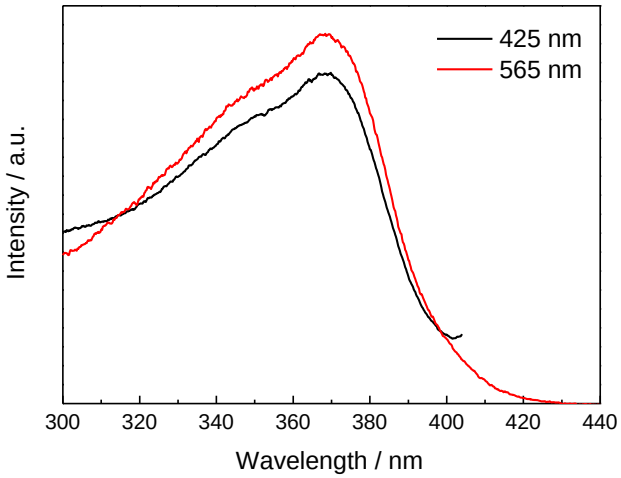

Fig. S6 Excitation spectra of **1ar** crystals. Excitation wavelengths were scanned with the emission wavelengths at 425 and 565 nm. These measurements were performed at room temperature.

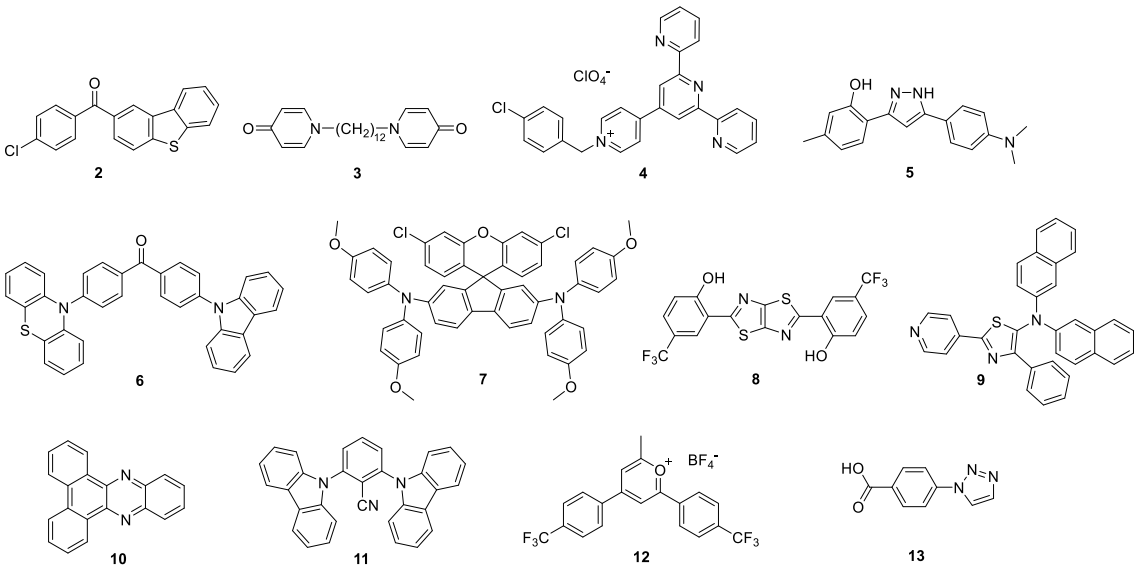

Fig. S7 Some examples of reported single-molecule white light emitters in solid state.[S19-S30]

Table S1. Emission quantum yields (Φ_{em}) and CIE1931 coordinates at room temperature of single-molecule white light emitters in solid state.

Compound	Φ_{em} (λ_{exc})	CIE1931 coordinates (x. y)	Emission composition	Ref.
2	0.072 (365 nm)	(0.33, 0.35)	Dual phosphorescence	S19
3	0.32 (365 nm)	(0.34, 0.36)	Fluorescence (monomer and excimer)	S20
4	0.12 (360 nm)	(0.32, 0.33)	Fluorescence (monomer and CT)	S21
5	0.13 (No data)	(0.313, 0.339)	Fluorescence (ESIPT)	S22
6	0.23 (No data)	(0.35, 0.35)	Fluorescence (AIE-DF)	S23
7[a]	0.0416 (365 nm)	(0.30, 0.30)	fluorescence (monomer and excimer)	S24
8	0.27 (No data)	No data	Fluorescence (ESIPT-excimer and MFC)	S25
9[b]	0.07 (365 nm)	(0.32, 0.33)	Fluorescence (MFC)	S26
10	0.01 (390 nm)	(0.28, 0.33)	Fluorescence and dual phosphorescence	S27
11	0.238 (360 nm)	(0.3133, 0.3578)[c]	Fluorescence and phosphorescence	S28
12	0.09 (340 nm)	(0.28, 0.36)	Fluorescence	S29
13	0.0204 (320 nm)	(0.31, 0.35)[d]	SAE	S30

[a] A film produced by the spin-coating method. [b] After the powder was ground, acetone was fumed. [c] λ_{ex} = 365 nm. [d] λ_{ex} = 370 nm.

Abbreviations for emission composition are: charge-transfer (CT), excited-state intramolecular proton transfer (ESIPT), aggregation-induced emission (AIE), delayed fluorescence (DF), mechanofluorochromism (MFC), and supramolecular aggregate emission (SAE), respectively.

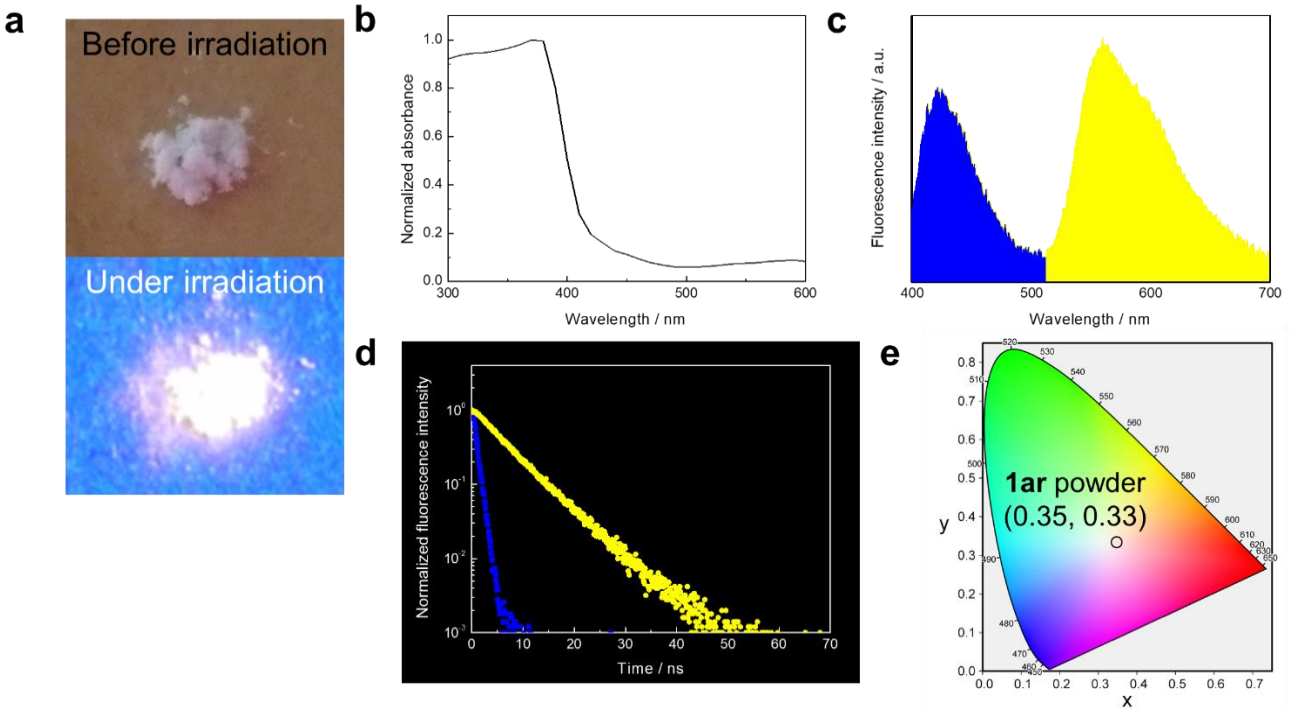

Fig. S8 (a) Photographs of fluorescence emission of **1ar** powder before (top) and under UV light (λ = 365 nm) irradiation (bottom). (b) Absorption spectrum of **1ar** powder. (c) Fluorescence spectrum of **1ar** powder (λ_{exc} = 340 nm). (d) Fluorescence decay curves of **1ar** powder at 425 (blue square: τ = 0.88 ns) and 565 nm (yellow circle: τ = 6.34 ns) emission (λ_{exc} = 340 nm). (e) CIE 1931 coordinates of emission of **1ar** powder (λ_{exc} = 340 nm). These observations and measurements were performed at room temperature.

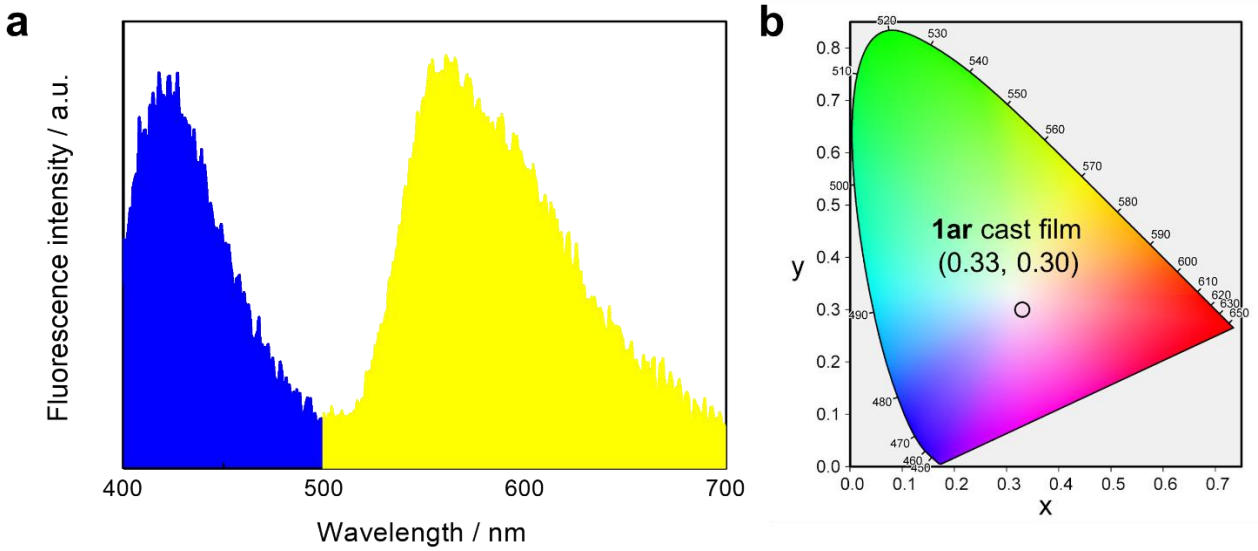

Fig. S9 (a) Fluorescence spectrum of **1ar** cast film (λ_{exc} = 340 nm). (b) CIE 1931 coordinates of emission of **1ar** cast film (λ_{exc} = 340 nm). These measurements were performed at room temperature.

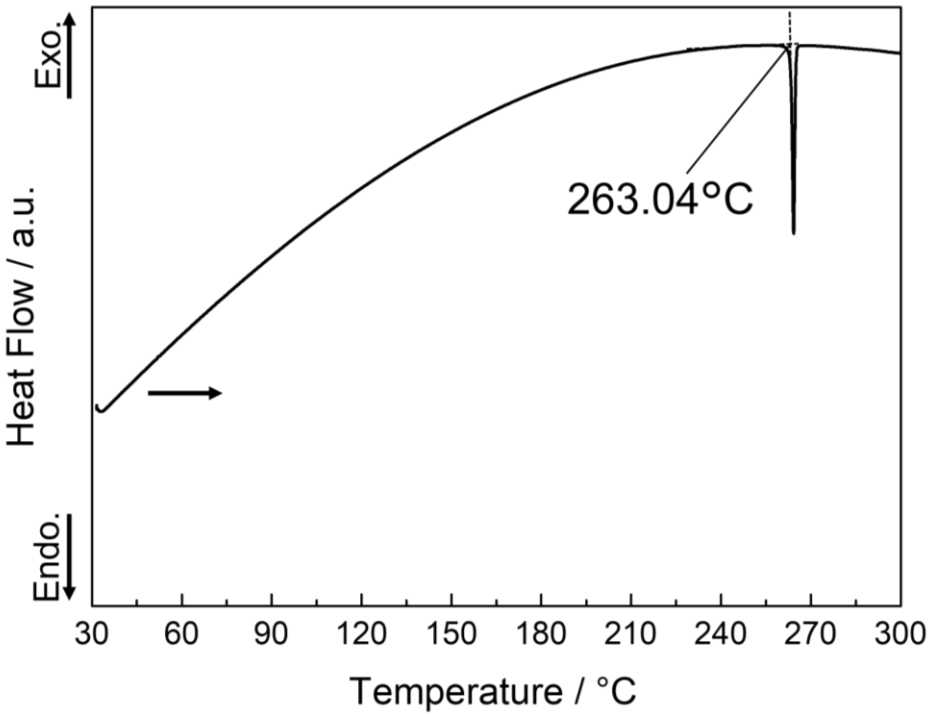

Fig. S10 DSC curve of **1ar** crystals. DSC trace at heating rate of 10 °C min^{-1}.

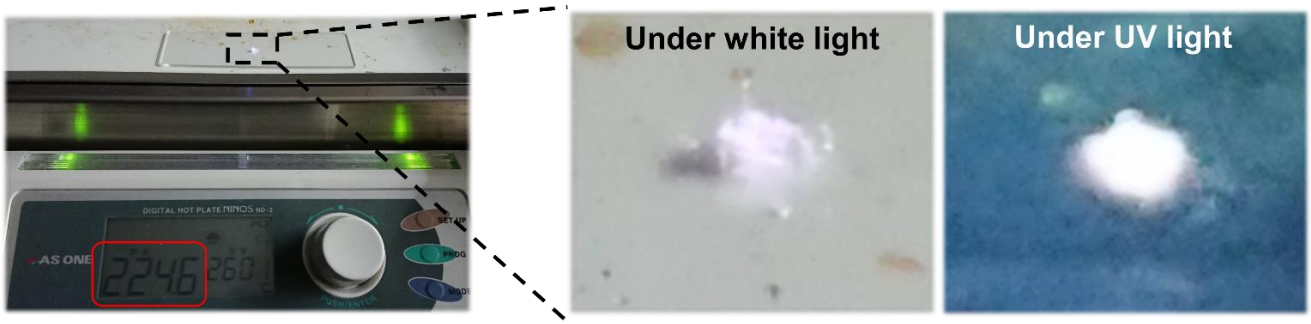

Fig. S11 Photographs of **1ar** powder under white light and UV (λ = 365 nm, 277 mW cm^{-2}) light irradiation at heating conditions above 224 °C. The light was irradiated from directly above.

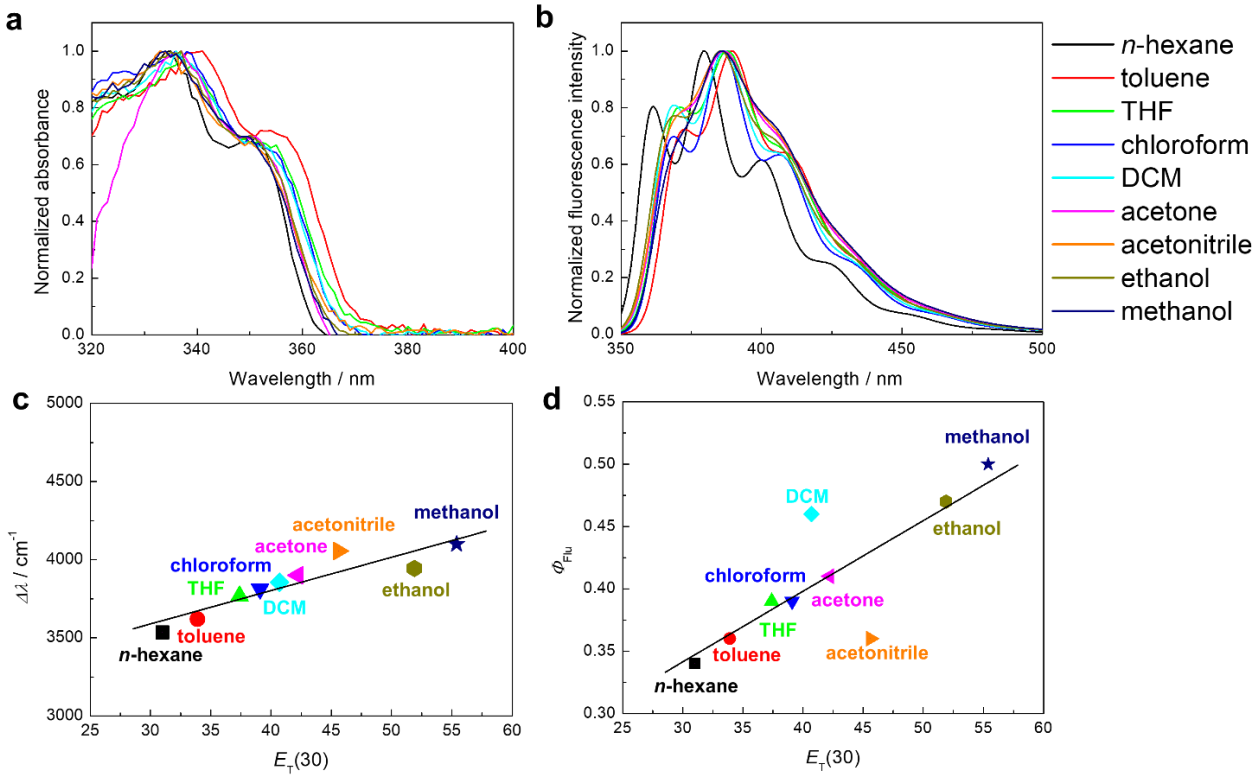

Fig. S12 (a, b) Normalized absorption (a) and fluorescence (b) spectra of **1ar** in nine kinds of solvents (λ_{exc} = 336 nm). (c) Plots of stokes shift vs. $E_T(30)$ **1ar** in the nine solvents. (d) Plots of fluorescence quantum yield vs. $E_T(30)$ of **1ar** in the nine solvents. These measurements were performed in dilute solution at room temperature.

Table S2. Optical properties of **1ar** in the nine kinds of solvents.

Solvent	$E_T(30)$ [kcal/mol]	λ^{max}_{Abs} [nm]	λ^{max}_{em} [nm]	$\Delta\lambda$ (λ^{max}_{em}-λ^{max}_{Abs}) [nm]	[cm^{-1}]	Φ_{Flu}[a] [%]
n-hexane	31.0	335	380	45	3535	33.8
toluene	33.9	341	389	48	3619	36.2
THF	37.4	337	386	49	3767	38.8
chloroform	39.1	338	388	50	3813	39.3
DCM	40.7	336	386	50	3855	45.8
acetone	42.2	337	388	51	3900	40.9
acetonitrile	45.6	333	385	52	4056	36.4
ethanol	51.9	335	386	51	3944	47.1
methanol	55.4	334	387	53	4100	49.8

[a] λ_{exc} = 336 nm.

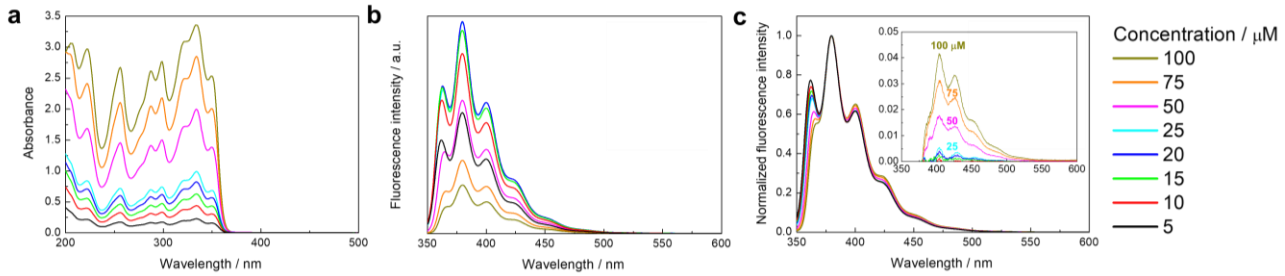

Fig. S13 (a, b) Absorption (a) and fluorescence (b) spectral changes with different concentrations of **1ar** in *n*-hexane (λ_{exc} = 336 nm). Absorbance increased with increasing concentration. Fluorescence intensity increased with increasing concentration from 5-20 μM, but fluorescence intensity decreased with increasing concentration above 25 μM due to concentration quenching. (c) Normalized fluorescence spectra with different concentrations of **1ar** in *n*-hexane. The difference spectra (inset) show the gradual appearance of red-shifted monomer emission due to intermolecular interactions with increasing concentration of **1ar**. The difference spectra were obtained from the difference between the spectra of 5 μM and other concentrations of **1ar**. These measurements were performed at room temperature.

Table S3. Crystal data of **1ar** prepared by recrystallization from solution in hexane.

	1ar
Formula	$C_{23}H_{10}F_6N_2S_2$
Formula weight	492.45
T / K	100(2)
Crystal system	triclinic
Space group	$P\bar{1}$
a / Å	7.5038(2)
b / Å	14.3528(5)
c / Å	19.3127(7)
α / °	77.5284(14)
β / °	83.8844(13)
γ / °	80.5922(13)
V / Å^3	1998.11(11)
Z	4
R_1 (I > 2σ(I))	0.0277
wR_2 (I > 2σ(I))	0.0690
R_1 (all data)	0.0345
wR_2 (all data)	0.0713
CCDC No.	2159901

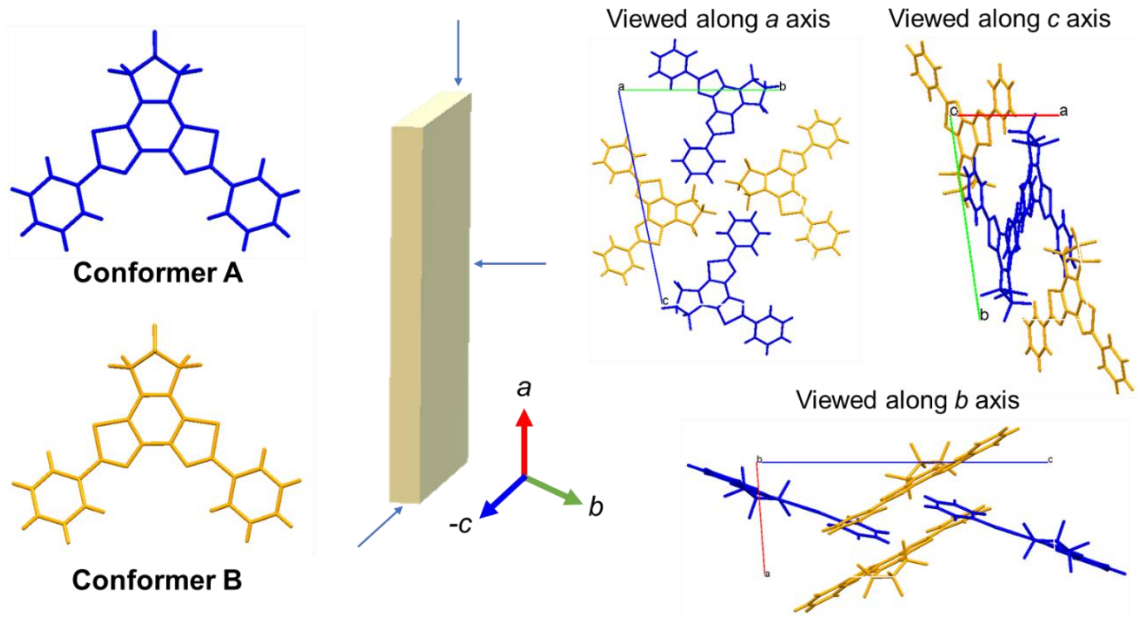

Fig. S14 Molecular packing of **1ar** in the crystal. There are two conformers (A and B) with a 1:1 ratio of **1ar** molecules in crystal. Conformers A and B are shown in blue and bright yellow, respectively.

Table S4. Geometric parameters of crystal and optimized structures of **1ar**.

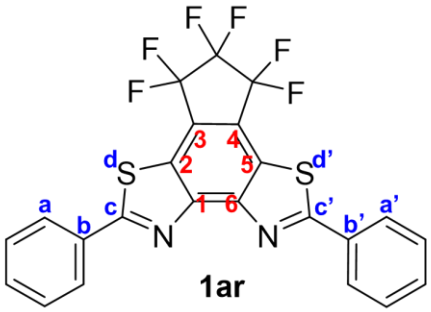

1ar

φ_1 = ∢(C_1, C_2, C_3, C_4), φ_2 = ∢(C_3, C_4, C_5, C_6)

θ_1 = ∢(C_a, C_b, C_c, C_d), θ_2 = ∢($C_{a'}$, $C_{b'}$, $C_{c'}$, $C_{d'}$)

	Conformer A		Conformer B	
	Crystal[a]	Optimized[b]	crystal[a]	Optimized[b]
$r_{C_1\text{-}C_6}$ [Å]	1.416	1.421	1.419	1.421
φ_1 [degree]	0.50	-0.4	1.51	-0.4
φ_2 [degree]	0.31	0.4	-1.89	0.4
θ_1 [degree]	-0.48	1.3	9.68	1.2
θ_2 [degree]	-13.02	-1.3	4.28	-1.2

[a] Geometric parameters of the crystal structure obtained from X-ray crystallographic analysis.
[b] Geometric parameters of optimized structure on the B3LYP/6-31G(d,p) level of theory.

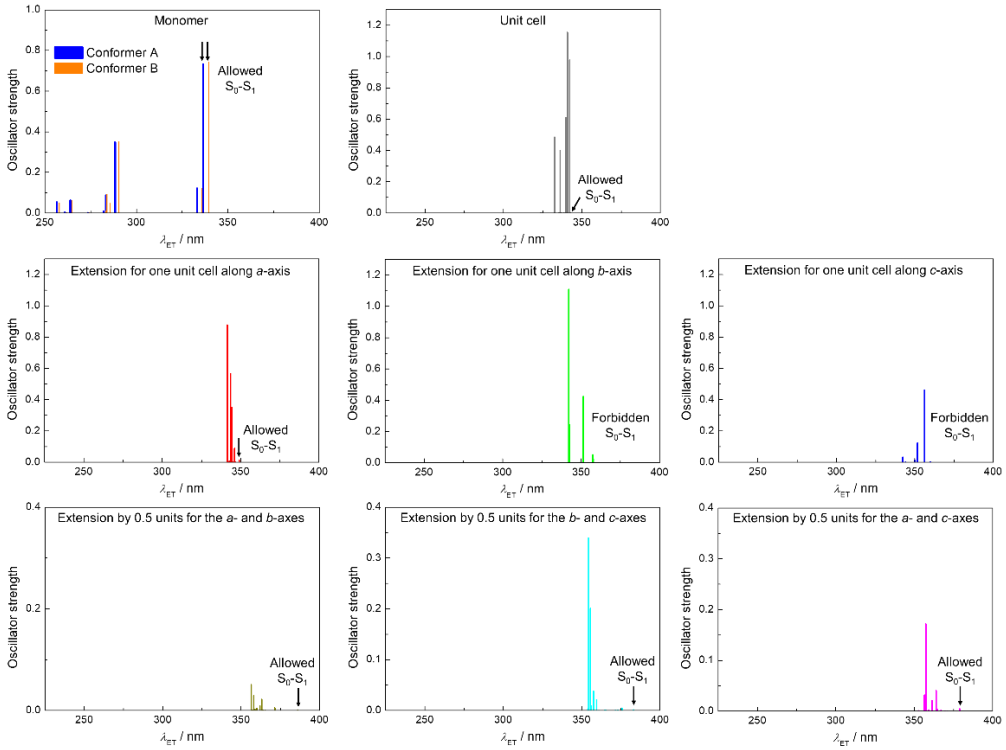

Fig. S15 Electronic transitions estimated for a single molecule, unit cell, and large supercell of **1ar** with geometries of crystal structure obtained from X-ray crystallographic analysis using the TD-DFT method based on the B3LYP/6-31G(d,p) level of theory.

Table S5. Results of TD-DFT calculations of a single molecule and unit cell of **1ar** with geometries of crystal structure obtained from X-ray crystallographic analysis.

	Single molecule		
Excited states	Conformer A	Conformer B	Unit cell
1st	336.44 nm (3.69 eV) *f* = 0.7323 HOMO→LUMO: 0.70	339.47 nm (3.65 eV) *f* = 0.7436 HOMO→LUMO: 0.70	342.69 nm (3.62 eV) *f* = 0.0005 HOMO-7→LUMO+1: -0.14 HOMO-6→LUMO: -0.14 HOMO-3→LUMO: 0.22 HOMO-3→LUMO+1: -0.15 HOMO-2→LUMO: -0.16 HOMO-2→LUMO+1: -0.22 HOMO-1→LUMO: -0.16 HOMO-1→LUMO+1: 0.23 HOMO-1→LUMO+2: 0.16 HOMO-1→LUMO+3: -0.18 HOMO→LUMO: 0.25 HOMO→LUMO+1: 0.15 HOMO→LUMO+2: -0.19 HOMO→LUMO+3: -0.17
2nd	333.14 nm (3.72 eV) *f* = 0.1214 HOMO-1→LUMO: 0.66 HOMO→LUMO+1: -0.22	335.90 nm (3.69 eV) *f* = 0.1210 HOMO-1→LUMO: 0.66 HOMO→LUMO+1: 0.22	342.27 nm (3.62 eV) *f* = 0.9779 HOMO-3→LUMO+1: 0.16 HOMO-2→LUMO: -0.15

	HOMO→LUMO+2: -0.10	HOMO→LUMO+2: 0.10	HOMO-1→LUMO: 0.23 HOMO-1→LUMO+1: -0.27 HOMO-1→LUMO+2: -0.21 HOMO-1→LUMO+3: 0.19 HOMO→LUMO: 0.27 HOMO→LUMO+1: 0.21 HOMO→LUMO+2: -0.18 HOMO→LUMO+3: -0.20
3rd	288.38 nm (4.30 eV) *f* = 0.3492 HOMO-2→LUMO: 0.17 HOMO-1→LUMO: 0.21 HOMO→LUMO+1: 0.64	290.51 nm (4.27 eV) *f* = 0.3507 HOMO-2→LUMO: -0.15 HOMO-1→LUMO: -0.21 HOMO→LUMO+1: 0.65	340.97 nm (3.64 eV) *f* = 0.0014 HOMO-3→LUMO: -0.25 HOMO-3→LUMO+1: 016 HOMO-2→LUMO: 0.18 HOMO-2→LUMO+1: 0.25 HOMO-1→LUMO: -0.19 HOMO-1→LUMO+1: 0.31 HOMO→LUMO: 0.32 HOMO→LUMO+1: 0.21
4th	283.68 nm (4.37 eV) *f* = 0.0635 HOMO-3→LUMO: -0.30 HOMO-2→LUMO: 0.20 HOMO-1→LUMO+1: 0.58	285.79 nm (4.34 eV) *f* = 0.0480 HOMO-3→LUMO: 0.16 HOMO-1→LUMO+1: 0.67	340.63 nm (3.64 eV) *f* = 1.1552 HOMO-3→LUMO+1: 0.18 HOMO-2→LUMO: -0.17 HOMO-1→LUMO: -0.21 HOMO-1→LUMO+1: 0.28 HOMO-1→LUMO+2: -0.23 HOMO-1→LUMO+3: 0.21 HOMO→LUMO: -0.25 HOMO→LUMO+1: -0.21 HOMO→LUMO+2: -0.21 HOMO→LUMO+3: -0.22
5th	283.33 nm (4.38 eV) *f* = 0.0869 HOMO-3→LUMO+1: -0.12 HOMO-2→LUMO: 0.61 HOMO-1→LUMO+1: -0.21 HOMO→LUMO+1: -0.14	283.89 nm (4.37 eV) *f* = 0.0925 HOMO-4→LUMO+1: 0.13 HOMO-2→LUMO: 0.64 HOMO-1→LUMO+4: -0.10 HOMO→LUMO+1: 0.12 HOMO→LUMO+5: -0.10	339.74 nm (3.65 eV) *f* = 0.6105 HOMO-3→LUMO: 0.11 HOMO-3→LUMO+1: -0.40 HOMO-2→LUMO: 0.40 HOMO-2→LUMO+1: 0.11 HOMO-1→LUMO+2: -0.18 HOMO-1→LUMO+3: 0.17 HOMO→LUMO+2: -0.17 HOMO→LUMO+3: -0.19
6th	282.03 nm (4.40 eV) *f* = 0.0077 HOMO-3→LUMO: 0.59 HOMO-2→LUMO+1: -0.11 HOMO-1→LUMO+1: 0.32 HOMO→LUMO+4: 0.10	283.19 nm (4.38 eV) *f* = 0.0080 HOMO-3→LUMO: 0.64 HOMO-2→LUMO+1: 0.13 HOMO-1→LUMO+1: -0.17 HOMO→LUMO+4: 0.12	338.62 nm (3.66 eV) *f* = 0.0000 HOMO-7→LUMO+1: 0.19 HOMO-6→LUMO: 0.19 HOMO-3→LUMO: 0.23 HOMO-3→LUMO+1: -0.16 HOMO-2→LUMO: -0.16 HOMO-2→LUMO+1: -0.23 HOMO-1→LUMO+1: 0.13 HOMO+1→LUMO+2: -0.22 HOMO-1→LUMO+3: 0.25 HOMO→LUMO+2: 0.24 HOMO→LUMO+3: 0.21
7th	273.49 nm (4.53 eV) *f* = 0.0006 HOMO-7→LUMO+1: -0.16	274.17 nm (4.52 eV) *f* = 0.0016 HOMO-7→LUMO+1: -0.16	337.00 nm (3.68 eV) *f* = 0.0002 HOMO→LUMO: -0.41

	HOMO-6→LUMO: 0.68	HOMO-6→LUMO: 0.68	HOMO→LUMO+1: 0.56
8th	263.83 nm (4.70 eV) *f* = 0.0624 HOMO-7→LUMO: 0.12 HOMO-4→LUMO: 0.62 HOMO-1→LUMO: 0.10 HOMO→LUMO+2: 0.25	264.92 nm (4.68 eV) *f* = 0.0628 HOMO-7→LUMO: 0.12 HOMO-4→LUMO: 0.62 HOMO-1→LUMO: -0.11 HOMO→LUMO+2: 0.26	336.99 nm (3.68 eV) *f* = 0.0002 HOMO-1→LUMO: 0.57 HOMO-1→LUMO+1: 0.40
9th	260.89 nm (4.75 eV) *f* = 0.0027 HOMO-7→LUMO: 0.62 HOMO-6→LUMO+1: -0.29 HOMO-4→LUMO: -0.11	261.83 nm (4.74 eV) *f* = 0.0024 HOMO-7→LUMO: 0.63 HOMO-6→LUMO+1: -0.29 HOMO-4→LUMO: -0.11	336.11 nm (3.69 eV) *f* = 0.4000 HOMO-7→LUMO: 0.40 HOMO-7→LUMO+1: -0.18 HOMO-6→LUMO: 0.18 HOMO-6→LUMO+1: 0.40 HOMO-3→LUMO+1: 0.12 HOMO-3→LUMO+5: -0.13 HOMO-2→LUMO: -0.12 HOMO-2→LUMO+4: 0.13
10th	256.42 nm (4.84 eV) *f* = 0.0535 HOMO-5→LUMO: 0.65 HOMO-1→LUMO+2: -0.21	257.77 nm (4.81 eV) *f* = 0.0503 HOMO-5→LUMO: 0.65 HOMO-1→LUMO+2: 0.20	335.24 nm (3.70 eV) *f* = 0.0000 HOMO-7→LUMO+1: 0.37 HOMO-6→LUMO: 0.37 HOMO-5→LUMO+2: 0.17 HOMO-4→LUMO+3: -0.17 HOMO-3→LUMO+4: -0.12 HOMO-2→LUMO+5: 0.12 HOMO-1→LUMO+2: 0.13 HOMO-1→LUMO+3: -0.15 HOMO→LUMO+2: -0.15 HOMO→LUMO+3: -0.13
11th	248.60 nm (4.99 eV) *f* = 0.0010 HOMO-3→LUMO: 0.19 HOMO-2→LUMO+1: 0.60 HOMO-1→LUMO+2: -0.19 HOMO→LUMO+3: 0.10 HOMO→LUMO+4: -0.15	249.06 nm (4.98 eV) *f* = 0.0019 HOMO-3→LUMO: -0.20 HOMO-2→LUMO+1: 0.59 HOMO-1→LUMO+2: -0.20 HOMO→LUMO+4: 0.17	332.50 nm (3.73 eV) *f* = 0.4846 HOMO-5→LUMO+2: 0.14 HOMO-5→LUMO+3: -0.43 HOMO-4→LUMO+2: 0.43 HOMO-4→LUMO+3: 0.15 HOMO-1→LUMO+6: -0.10 HOMO-1→LUMO+7: 0.11 HOMO→LUMO+6: 0.11 HOMO→LUMO+7: 0.10
12th	247.58 nm (5.01 eV) *f* = 0.0015 HOMO-3→LUMO+1: 0.59 HOMO-2→LUMO: 0.19 HOMO-1→LUMO+4: 0.14 HOMO→LUMO+2: 0.20 HOMO→LUMO+5: -0.16	248.16 nm (5.00 eV) *f* = 0.0019 HOMO-3→LUMO+1: 0.58 HOMO-2→LUMO: -0.20 HOMO-1→LUMO+4: -0.13 HOMO→LUMO+2: 0.20 HOMO→LUMO+5: -0.17	332.13 nm (3.73 eV) *f* = 0.0001 HOMO-7→LUMO+1: -0.11 HOMO-6→LUMO: -0.11 HOMO-5→LUMO+2: 0.39 HOMO-5→LUMO+3: -0.15 HOMO-4→LUMO+2: -0.13 HOMO-4→LUMO+3: -0.39 HOMO-1: LUMO+2: -0.11 HOMO-1→LUMO+3: 0.13 HOMO→LUMO+2: 0.13 HOMO→LUMO+3: 0.11
13th	240.46 nm (5.16 eV) *f* = 0.1522 HOMO-5→LUMO: 0.15 HOMO-4→LUMO+1: 0.24	241.50 nm (5.13 eV) *f* = 0.1437 HOMO-5→LUMO: -0.14 HOMO-4→LUMO+1: -0.23	324.06 nm (3.83 eV) *f* = 0.0012 HOMO-5→LUMO: -0.21 HOMO-5→LUMO+1: -0.22

	HOMO-2→LUMO+1: 0.16 HOMO-1→LUMO+2: 0.50 HOMO→LUMO+3: -0.31 HOMO→LUMO+4: -0.13	HOMO-2→LUMO+1: 0.17 HOMO-1→LUMO+2: 0.49 HOMO→LUMO+3: 0.33 HOMO→LUMO+4: 0.52	HOMO-4→LUMO: 0.51 HOMO-4→LUMO+1: 0.33
14th	240.15 nm (5.16 eV) *f* = 0.0071 HOMO-4→LUMO: -0.25 HOMO-3→LUMO+1: -0.17 HOMO-1→LUMO+3: 0.28 HOMO→LUMO+2: 0.54	241.19 nm (5.14 eV) *f* = 0.0105 HOMO-4→LUMO: -0.25 HOMO-3→LUMO+1: -0.19 HOMO-1→LUMO+3: -0.29 HOMO→LUMO+2: 0.52	324.04 nm (3.83 eV) *f* = 0.0008 HOMO-5→LUMO: -0.38 HOMO-5→LUMO+1: 0.48 HOMO-4→LUMO: -0.13 HOMO-4→LUMO+1: 0.28
15th	232.00 nm (5.34 eV) *f* = 0.0010 HOMO-7→LUMO: 0.30 HOMO-6→LUMO+1: 0.63	232.45 nm (5.33 eV) *f* = 0.0094 HOMO-7→LUMO: 0.29 HOMO-6→LUMO+1: 0.62 HOMO-4→LUMO+1: 0.11	323.41 nm (3.83 eV) *f* = 0.0000 HOMO-5→LUMO: 0.18 HOMO-5→LUMO+1: -0.24 HOMO-4→LUMO: -0.36 HOMO-4→LUMO+1: 0.51

Table S6. Results of TD-DFT calculations of the large supercell extended by one unit cell along one axis of **1ar** with geometries of crystal structure obtained from X-ray crystallographic analysis.

	Extension for one unit cell along one axis		
Excited states	*a*	*b*	*c*
1st	349.18 nm (3.55 eV) *f* = 0.0121 HOMO-1→LUMO: -0.16 HOMO→LUMO: 0.67	380.26 nm (3.26 eV) *f* = 0.0000 HOMO-2→LUMO: -0.20 HOMO→LUMO: 0.67	374.73 nm (3.31 eV) *f* = 0.0000 HOMO→LUMO+2:0.70
2nd	349.15 nm (3.55 eV) *f* = 0.0098 HOMO-1→LUMO+1: 0.67 HOMO→LUMO+2: 0.16	357.78 nm (3.47 eV) *f* = 0.0236 HOMO-11→LUMO: 0.21 HOMO-5→LUMO: -0.37 HOMO-1→LUMO: 0.34 HOMO→LUMO+5: 0.42	359.76 nm (3.45 eV) *f* = 0.0015 HOMO→LUMO: 0.49 HOMO→LUMO+1: 0.51
3rd	346.58 nm (3.58 eV) *f* = 0.0000 HOMO-9→LUMO+1: 0.12 HOMO-8→LUMO: 0.12 HOMO-5→LUMO+2: 0.12 HOMO-5→LUMO+3: 0.29 HOMO-4→LUMO+2: 0.30 HOMO-4→LUMO+3: -0.11 HOMO-3→LUMO+2: 0.18 HOMO-3→LUMO+3: -0.10 HOMO-3→LUMO+4: 0.25 HOMO-2→LUMO+2: -0.11 HOMO-2→LUMO+3: -0.15 HOMO-2→LUMO+5: 0.25 HOMO→LUMO+7: -0.10	357.31 nm (3.47 eV) *f* = 0.0515 HOMO-5→LUMO: 0.29 HOMO-4→LUMO: -0.13 HOMO-2→LUMO: 0.11 HOMO-1→LUMO: 0.57 HOMO→LUMO+5: -0.17	359.73 nm (3.45 eV) *f* = 0.0001 HOMO→LUMO: 0.50 HOMO→LUMO+1: -0.49

4th	346.05 nm (3.58 eV) *f* = 0.0873 HOMO-9→LUMO+1: -0.16 HOMO-8→LUMO: 0.16 HOMO-5→LUMO+2: 0.27 HOMO-5→LUMO+3: -0.13 HOMO-4→LUMO+2: 0.13 HOMO-4→LUMO+3: 0.28 HOMO-3→LUMO+3: 0.21 HOMO-3→LUMO+5: -0.19 HOMO-2→LUMO+2: -0.22 HOMO-2→LUMO+4: -0.19 HOMO-1→LUMO+6: 0.10 HOMO-1→LUMO+7: 0.13 HOMO→LUMO+6: 0.13	357.26 nm (3.47 eV) *f* = 0.0023 HOMO-3→LUMO: 0.15 HOMO-2→LUMO: 0.65 HOMO→LUMO: 0.18	356.10 nm (3.48 eV) *f* = 0.4611 HOMO-7→LUMO+2: 0.16 HOMO-1→LUMO+2: 0.62 HOMO→LUMO+7: -0.25
5th	345.04 nm (3.59 eV) *f* = 0.0000 HOMO-5→LUMO+3: 0.18 HOMO-4→LUMO+2: 0.19 HOMO-3→LUMO+4: -0.16 HOMO-2→LUMO+5: -0.16 HOMO-1→LUMO+6: 0.35 HOMO-1→LUMO+7: 0.17 HOMO→LUMO+6: -0.17 HOMO→LUMO+7: 0.35	351.39 nm (3.53 eV) *f* = 0.4241 HOMO-11→LUMO: 0.30 HOMO-5→LUMO: 0.47 HOMO-2→LUMO+5: -0.11 HOMO-1→LUMO: -0.12 HOMO→LUMO+5: 0.35	353.25 nm (3.51 eV) *f* = 0.0000 HOMO-4→LUMO+2: 0.16 HOMO-2→LUMO+2: 0.66
6th	344.23 nm (3.60 eV) *f* = 0.3505 HOMO-3→LUMO+2: -0.11 HOMO-3→LUMO+3: -0.35 HOMO-2→LUMO+2: 0.39 HOMO-1→LUMO+6: 0.17 HOMO-1→LUMO+7: 0.22 HOMO→LUMO+6: 0.22 HOMO→LUMO+7: -0.17	349.10 nm (3.55 eV) *f* = 0.0001 HOMO-3→LUMO+1: 0.11 HOMO-2→LUMO+1: 0.40 HOMO-1→LUMO+1: 0.50 HOMO→LUMO+1: 0.24	351.83 nm (3.52 eV) *f* = 0.1221 HOMO-7→LUMO+2: 0.61 HOMO-2→LUMO+1: -0.11 HOMO-1→LUMO: -0.15 HOMO-1→LUMO+2: -0.18 HOMO→LUMO+7: -0.14
7th	344.03 nm (3.60 eV) *f* = 0.0029 HOMO-9→LUMO+1: 0.11 HOMO-8→LUMO: 0.11 HOMO-5→LUMO+3: 0.19 HOMO-4→LUMO+2: 0.19 HOMO-3→LUMO+2: -0.35 HOMO-3→LUMO+3: 0.24 HOMO-2→LUMO+2: 0.22 HOMO-2→LUMO+3: 0.39	349.07 nm (3.55 eV) *f* = 0.0001 HOMO-4→LUMO+2: -0.11 HOMO-2→LUMO+2: -0.45 HOMO-1→LUMO+2: 0.45 HOMO→LUMO+2: -0.24	351.40 nm (3.53 eV) *f* = 0.0002 HOMO-2→LUMO: 0.37 HOMO-2→LUMO+1: -0.16 HOMO-1→LUMO: 0.30 HOMO-1→LUMO+1: 0.47
8th	343.68 nm (3.61 eV) *f* = 0.5650 HOMO-9→LUMO+1: -0.13 HOMO-8→LUMO: 0.12 HOMO-5→LUMO+2: 0.25 HOMO-5→LUMO+3: -0.13 HOMO-4→LUMO+2: 0.12 HOMO-4→LUMO+3: 0.26 HOMO-3→LUMO+3: -0.19 HOMO-2→LUMO+2: 0.20 HOMO-1→LUMO+6: -0.18 HOMO-1→LUMO+7: -0.24 HOMO→LUMO+6: -0.23 HOMO→LUMO+7: 0.18	348.71 nm (3.56 eV) *f* = 0.0007 HOMO-2→LUMO+2: 0.12 HOMO-2→LUMO+3: -0.14 HOMO→LUMO+2: -0.14 HOMO→LUMO+3: 0.63 HOMO→LUMO+4: 0.19	351.36 nm (3.53 eV) *f* = 0.0170 HOMO-7→LUMO+2: 0.19 HOMO-2→LUMO: 0.15 HOMO-2→LUMO+1: 0.36 HOMO-1→LUMO: 0.44 HOMO-1→LUMO+1: -0.29 HOMO-1→LUMO+2: 0.12

9th	342.84 nm (3.62 eV) *f* = 0.0040 HOMO-1→LUMO+2: -0.19 HOMO→LUMO+2: 0.61 HOMO→LUMO+3: 0.26	348.68 nm (3.56 eV) *f* = 0.0006 HOMO-2→LUMO+1: 0.10 HOMO-2→LUMO+4: -0.14 HOMO→LUMO+1: -0.14 HOMO→LUMO+3: -0.19 HOMO→LUMO+4: 0.63	349.95 nm (3.54 eV) *f* = 0.0057 HOMO-11→LUMO: 0.12 HOMO-6→LUMO: -0.13 HOMO-6→LUMO+1: 0.20 HOMO-5→LUMO+1: 0.13
10th	342.81 nm (3.62 eV) *f* = 0.0076 HOMO-1→LUMO+2: -0.23 HOMO-1→LUMO+3: 0.62 HOMO→LUMO+2: -0.17 HOMO→LUMO+3: 0.11	346.99 nm (3.57 eV) *f* = 0.0000 HOMO-10→LUMO: 0.66 HOMO-3→LUMO: 0.15	349.94 nm (3.54 eV) *f* = 0.0130 HOMO-10→LUMO+1: 0.12 HOMO-6→LUMO: -0.13 HOMO-5→LUMO: -0.20 HOMO-5→LUMO+1: 0.65
11th	342.59 nm (3.62 eV) *f* = 0.0039 HOMO-3→LUMO+1: -0.41 HOMO-2→LUMO+1: 0.56	344.33 nm (3.60 eV) *f* = 0.0000 HOMO-2→LUMO+1: -0.23 HOMO→LUMO+1: 0.64 HOMO→LUMO+4: 0.16	344.15 nm (3.60 eV) *f* = 0.0011 HOMO-7→LUMO: -0.39 HOMO-7→LUMO+1: -0.12 HOMO-2→LUMO: 0.40 HOMO-2→LUMO+1: 0.13 HOMO-1→LUMO: -0.36 HOMO-1→LUMO+1: -0.10
12th	342.57 nm (3.62 eV) *f* = 0.0034 HOMO-3→LUMO: 0.56 HOMO-2→LUMO: 0.41	344.33 nm (3.60 eV) *f* = 0.0000 HOMO-2→LUMO+2: -0.23 HOMO→LUMO+2: 0.64 HOMO→LUMO+3: 0.16	344.14 nm (3.60 eV) *f* = 0.0009 HOMO-7→LUMO: 0.11 HOMO-7→LUMO+1: 0.39 HOMO-2→LUMO: -0.13 HOMO-2→LUMO+1: 0.40 HOMO-1→LUMO: -0.11 HOMO-1→LUMO+1: 0.36
13th	341.89 nm (3.63 eV) *f* = 0.0003 HOMO-5→LUMO: 0.47 HOMO-4→LUMO: 0.51	342.62 nm (3.62 eV) *f* = 0.2407 HOMO-11→LUMO: -0.50 HOMO-9→LUMO+1: -0.14 HOMO-8→LUMO+2: 0.14 HOMO-7→LUMO+1: 0.11 HOMO-6→LUMO+2: -0.12 HOMO-5→LUMO: 0.10 HOMO-4→LUMO: 0.13 HOMO→LUMO+5: 0.29 HOMO→LUMO+12: -0.13	342.32 nm (3.62 eV) *f* = 0.0001 HOMO-13→LUMO: 0.27 HOMO-12→LUMO+1: 0.27 HOMO-6→LUMO+6: -0.13 HOMO-5→LUMO+5: -0.12 HOMO-4→LUMO+4: -0.24 HOMO-3→LUMO+3: 0.26 HOMO-2→LUMO+4: 0.14 HOMO-1→LUMO+3: -0.14 HOMO→LUMO+4: 0.35
14th	341.87 nm (3.63 eV) *f* = 0.0003 HOMO-5→LUMO+1: 0.51 HOMO-4→LUMO+1: -0.47	342.13 nm (3.62 eV) *f* = 1.1076 HOMO-13→LUMO+2: 0.13 HOMO-12→LUMO+1: -0.13 HOMO-9→LUMO+1: 0.29 HOMO-9→LUMO+4: -0.13 HOMO-8→LUMO+2: -0.28 HOMO-8→LUMO+3: 0.13 HOMO-7→LUMO+3: 0.10 HOMO-7→LUMO+4: -0.24 HOMO-6→LUMO+3: 0.24 HOMO-5→LUMO: 0.10 HOMO-2→LUMO+6: 0.16 HOMO-1→LUMO+7: -0.17	342.22 nm (3.62 eV) *f* = 0.0323 HOMO-3→LUMO+4: 0.11 HOMO-2→LUMO+3: 0.14 HOMO-1→LUMO+4: -0.19 HOMO→LUMO+3: 0.63

15th	341.46 nm (3.63 eV) *f* = 0.8768 HOMO-3→LUMO+2: 0.16 HOMO-3→LUMO+3: 0.32 HOMO-3→LUMO+5: 0.33 HOMO-2→LUMO+2: 0.18 HOMO-2LUMO+3: -0.17 HOMO-2→LUMO+4: 0.32 HOMO-1→LUMO+7: 0.10 HOMO→LUMO+6: 0.10	341.62 nm (3.63 eV) *f* = 0.0001 HOMO-2→LUMO+2: -0.11 HOMO-2→LUMO+3: 0.40 HOMO-2→LUMO+4: 0.15 HOMO-1→LUMO+2: -0.13 HOMO-1→LUMO+3: 0.49 HOMO-1→LUMO+4: 0.18	342.05 nm (3.63 eV) *f* = 0.0034 HOMO-13→LUMO: -0.21 HOMO-12→LUMO+1: -0.19 HOMO-6→LUMO+6: 0.14 HOMO-5→LUMO+5: 0.11 HOMO-4→LUMO+4: 0.15 HOMO-3→LUMO+3: -0.14 HOMO-1→LUMO+3: -0.13 HOMO→LUMO+4: 0.55

Table S7. Results of TD-DFT calculations of the large supercell extended by 0.5 unit cells for two axes of **1ar** with geometries of crystal structure obtained from X-ray crystallographic analysis.

	Extension by 0.5 units for two axes		
Excited states	*a* and *b*	*b* and *c*	*a* and *c*
1st	386.33 nm (3.21 eV) *f* = 0.0010 HOMO→LUMO+3: 0.57 HOMO→LUMO+4: 0.19 HOMO→LUMO+5: -0.34	382.91 nm (3.24 eV) *f* = 0.0011 HOMO-1→LUMO+2: 0.68	378.97 nm (3.27 eV) *f* = 0.0046 HOMO→LUMO+3: 0.69
2nd	371.28 nm (3.34 eV) *f* = 0.0051 HOMO-1→LUIMO+3: 0.54 HOMO-1→LUMO+4: 0.18 HOMO-1→LUMO+5: -0.30 HOMO-1→LUMO+7: 0.21 HOMO-1→LUMO+8: 0.13	375.84 nm (3.30 eV) *f* = 0.0044 HOMO→LUMO+5: 0.67 HOMO→LUMO+6: -0.12	370.98 nm (3.34 eV) *f* = 0.0002 HOMO→LUMO: 0.70
3rd	365.61 nm (3.39 eV) *f* = 0.0000 HOMO→LUMO: 0.70	373.14 nm (3.32 eV) *f* = 0.0003 HOMO→LUMO: 0.69	369.53 nm (3.36 eV) *f* = 0.0006 HOMO→LUMO+1: 0.70
4th	365.33 nm (3.39 eV) *f* = 0.0000 HOMO→LUMO+1: 0.66 HOMO→LUMO+2: -0.24	371.44 nm (3.34 eV) *f* = 0.0003 HOMO→LUMO+1: 0.70	366.93 nm (3.38 eV) *f* = 0.0018 HOMO→LUMO+2: 0.70
5th	364.07 nm (3.41 eV) *f* = 0.0003 HOMO→LUMO+1: 0.24 HOMO→LUMO+2: 0.65	365.36 nm (3.39 eV) *f* = 0.0008 HOMO-2→LUMO: 0.66 HOMO-1→LUMO: -0.23	364.82 nm (3.40 eV) *f* = 0.0032 HOMO-4→LUMO: -0.17 HOMO-3→LUMO: -0.18 HOMO-1→LUMO: 0.64 HOMO-1→LUMO+3: 0.13
6th	363.16 nm (3.41 eV) *f* = 0.0213 HOMO-3→LUMO+3: -0.11 HOMO-2→LUMO+3: 0.53 HOMO-2→LUMO+4: 0.18 HOMO-2→LUMO+5: -0.30 HOMO-2→LUMO+7: 0.17 HOMO-1→LUMO+8: -0.10 HOMO→LUMO+7: -0.10	364.40 nm (3.40 eV) *f* = 0.0001 HOMO-2→LUMO+2: -0.19 HOMO→LUMO+2: 0.65	364.27 nm (3.40 eV) *f* = 0.0015 HOMO-4→LUMO+1: -0.12 HOMO-3→LUMO+1: -0.13 HOMO-1→LUMO+1: 0.66 HOMO-1→LUMO+3: -0.12

7th	361.84 nm (3.43 eV) *f* = 0.0086 HOMO-2→LUMO+5: 0.13 HOMO-1→LUMO+3: 0.22 HOMO-1→LUMO+4: 0.14 HOMO-1→LUMO+5: 0.48 HOMO→LUMO+3: -0.16 HOMO→LUMO+4: -0.10 HOMO→LUMO+5: -0.34	360.90 nm (3.44 eV) *f* = 0.0001 HOMO-2→LUMO: 0.23 HOMO-1→LUMO: 0.67	363.87 nm (3.41 eV) *f* = 0.0406 HOMO-1→LUMO: -0.13 HOMO-1→LUMO+1: 0.16 HOMO-1→LUMO+3: 0.51 HOMO→LUMO+7: -0.39
8th	360.33 nm (3.44 eV) *f* = 0.0003 HOMO-1→LUMO+1: 0.69 HOMO-1→LUMO+2: -0.10	359.41 nm (3.45 eV) *f* = 0.0082 HOMO-5→LUMO+2: 0.16 HOMO-4→LUMO+1: -0.11 HOMO-3→LUMO+1: 0.56 HOMO-2→LUMO+1: 0.18 HOMO-1→LUMO+1: 0.19 HOMO-1→LUMO+6: 0.21	361.23 nm (3.43 eV) *f* = 0.0214 HOMO-3→LUMO+7: -0.10 HOMO-1→LUMO+3: 0.41 HOMO→LUMO+7: 0.54
9th	359.94 nm (3.44 eV) *f* = 0.0038 HOMO-5→LUMO+3: 0.11 HOMO-3→LUMO+3: 0.12 HOMO-1→LUMO+5: -0.11 HOMO-1→LUMO+7: 0.14 HOMO→LUMO+5: -0.10 HOMMO→LUMO+7: 0.59	359.34 nm (3.45 eV) *f* = 0.0210 HOMO-9: LUMO+2: 0.17 HOMO-5→LUMO+2: 0.32 HOMO-4→LUMO+2: 0.15 HOMO-3→LUMO+1: -0.28 HOMO-3→LUMO+2: -0.14 HOMO-1→LUMO+5: 0.12 HOMO-1→LUMO+6: 0.43	359.24 nm (3.45 eV) *f* = 0.0025 HOMO-5→LUMO: 0.70
10th	358.81 nm (3.46 eV) *f* = 0.0003 HOMO-1→LUMO: 0.64 HOMO-1→LUMO+5: 0.11 HOMO→LUMO+3: 0.10 HOMO→LUMO+5: 0.20	357.38 nm (3.47 eV) *f* = 0.0375 HOMO-3→LUMO+2: -0.10 HOMO-2→LUMO+2: 0.42 HOMO-2→LUMO+5: 0.46 HOMO-1→LUMO+5: -0.14 HOMO→LUMO+2: 0.15	357.22 nm (3.47 eV) *f* = 0.1716 HOMO-6→LUMO+3: -0.12 HOMO-3→LUMO: 0.29 HOMO-3→LUMO+3: 0.55 HOMO→LUMO+8: 0.18
11th	358.67 nm (3.46 eV) *f* = 0.0017 HOMO-3→LUMO+3: 0.14 HOMO-1→LUMO: -0.28 HOMO-1→LUMO+2: 0.15 HOMO-1→LUMO+3: 0.15 HOMO-1→LUMO+5: 0.28 HOMO→LUMO+3: 0.20 HOMO→LUMO+4: 0.12 HOMO→LUMO+5: 0.41 HOMO→LUMO+7: 0.11 HOMO→LUMO+8: 0.12	356.16 nm (3.48 eV) *f* = 0.0085 HOMO-3→LUMO+1: -0.15 HOMO-2→LUMO+1: -0.23 HOMO-2→LUMO+2: -0.10 HOMO-1→LUMO+1: 0.61 HOMO-1→LUMO+4: -0.13	356.88 nm (3.47 eV) *f* = 0.0025 HOMO-6→LUMO+2: 0.10 HOMO-4→LUMO+2: 0.19 HOMO-1→LUMO+2: 0.66
12th	358.57 nm (3.46 eV) *f* = 0.0002 HOMO-2→LUMO+2: -0.27 HOMO-1→LUMO+1: 0.13 HOMO-1→LUMO+2: 0.61	356.08 nm (3.48 eV) *f* = 0.0072 HOMO-4→LUMO: 0.51 HOMO-3→LUMO: 0.45 HOMO-1→LUMO+1: -0.10	356.56 nm (3.48 eV) *f* = 0.0317 HOMO-6→LUMO: -0.12 HOMO-4→LUMO: 0.12 HOMO-3→LUMO: 0.57 HOMO-3→LUMO+3: -0.28 HOMO-1→LUIMO: 0.17
13th	357.83 nm (3.46 eV) *f* = 0.0286 HOMO-3→LUMO+3: 0.21 HOMO-3→LUMO+5: -0.15 HOMO→LUMO+5: -0.13 HOMO→LUMO+7: -0.15 HOMO→LUMO+8: 0.57	355.63 nm (3.49 eV) *f* = 0.2005 HOMO-9→LUMO+2: 0.11 HOMO-3→LUMO+2: 0.11 HOMO-2→LUMO+2: -0.40 HOMO-2→LUMO+5: 0.44 HOMO-1→LUMO+1: -0.11 HOMO-1→LUMO+6: 0.16 HOMO→LUMO+7: -0.11	353.17 nm (3.51 eV) *f* = 0.0001 HOMO-4→LUMO+1: 0.30 HOMO-3→LUMO+1: 0.59 HOMO-2→LUMO+1: 0.14 HOMO-1→LUMO+1: 0.17

14th	357.28 nm (3.47 eV) *f* = 0.0004 HOMO→LUMO+3: -0.25 HOMO→LUMO+4: 0.64	354.46 nm (3.50 eV) *f* = 0.3393 HOMO-9→LUMO+2: 0.11 HOMO-5→LUMO+2: -0.19 HOMO-4→LUMO+2: -0.20 HOMO-4→LUMO+5: -0.20 HOMO-3→LUMO+2: 0.24 HOMO-3→LUMO+5: 0.33 HOMO-2→LUMO+2: 0.26 HOMO-1→LUMO+5: 0.17 HOMO-1→LUMO+6: 0.23	352.76 nm (3.51 eV) *f* = 0.0000 HOMO-3→LUMO: -0.11 HOMO-2→LUMO: 0.70
15th	356.23 nm (3.48 eV) *f* = 0.0506 HOMO-3→LUMO+3: 0.43 HOMO-3→LUMO+4: 0.14 HOMO-3→LUMO+5: -0.26 HOMO-1→LUMO+7: 0.12 HOMO-2→LUMO+7: 0.10 HOMO-1→LUMO+7: -0.24 HOMO→LUMO+8: -0.29	353.96 nm (3.50 eV) *f* = 0.3393 HOMO-1→LUMO+3: 0.68 HOMO→LUMO+3: 0.11	352.48 nm (3.52 eV) *f* = 0.0008 HOMO-6→LUMO+2: 0.11 HOMO-4→LUMO+2: -0.40 HOMO-3→LUMO+2: 0.55

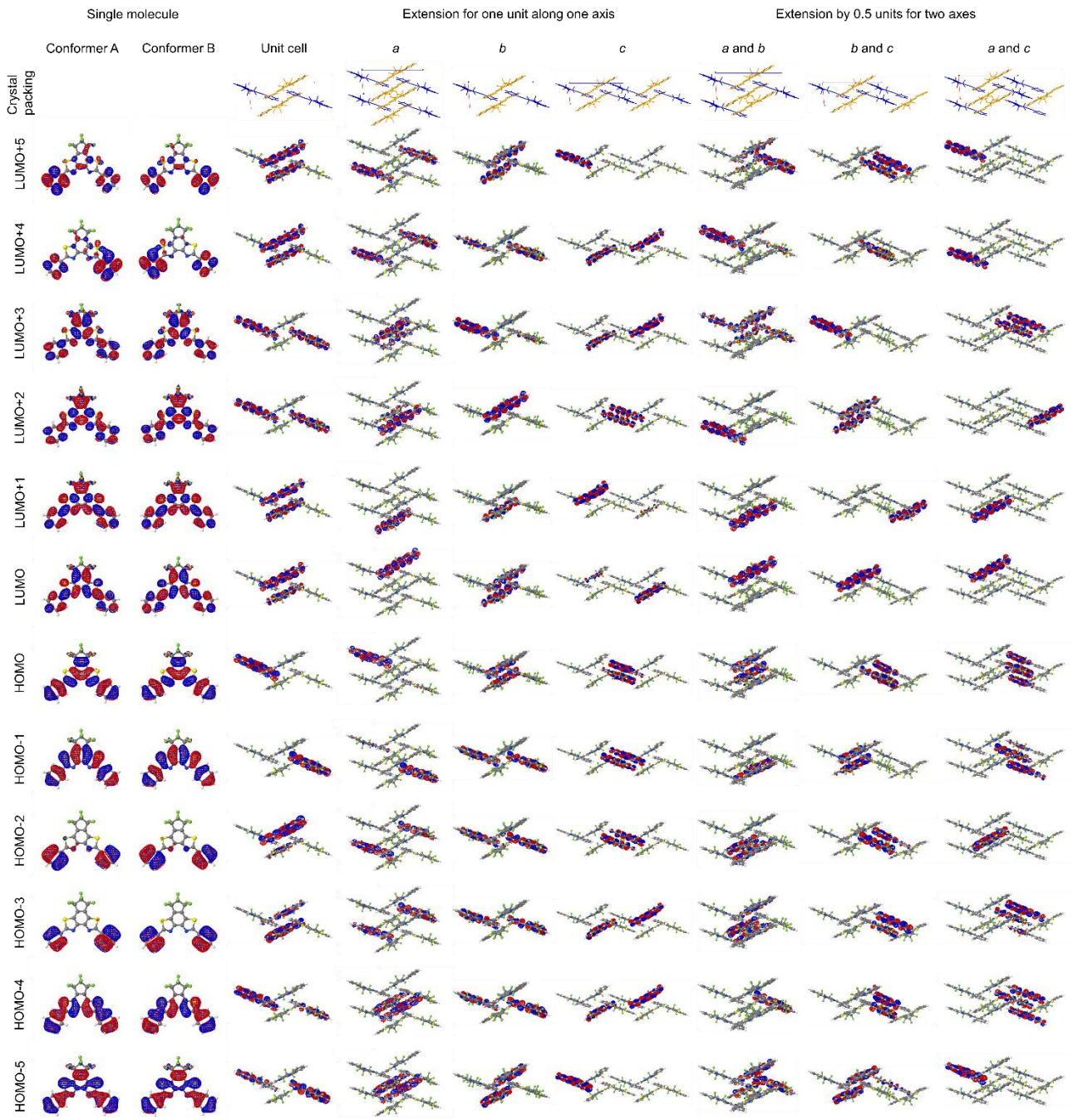

Fig. S16 Kohn-Sham molecular orbitals estimated for a single molecule, unit cell, and large supercell of **1ar** with geometries of crystal structure obtained from X-ray crystallographic analysis using the TD-DFT method based on the B3LYP/6-31G(d,p) level of theory.

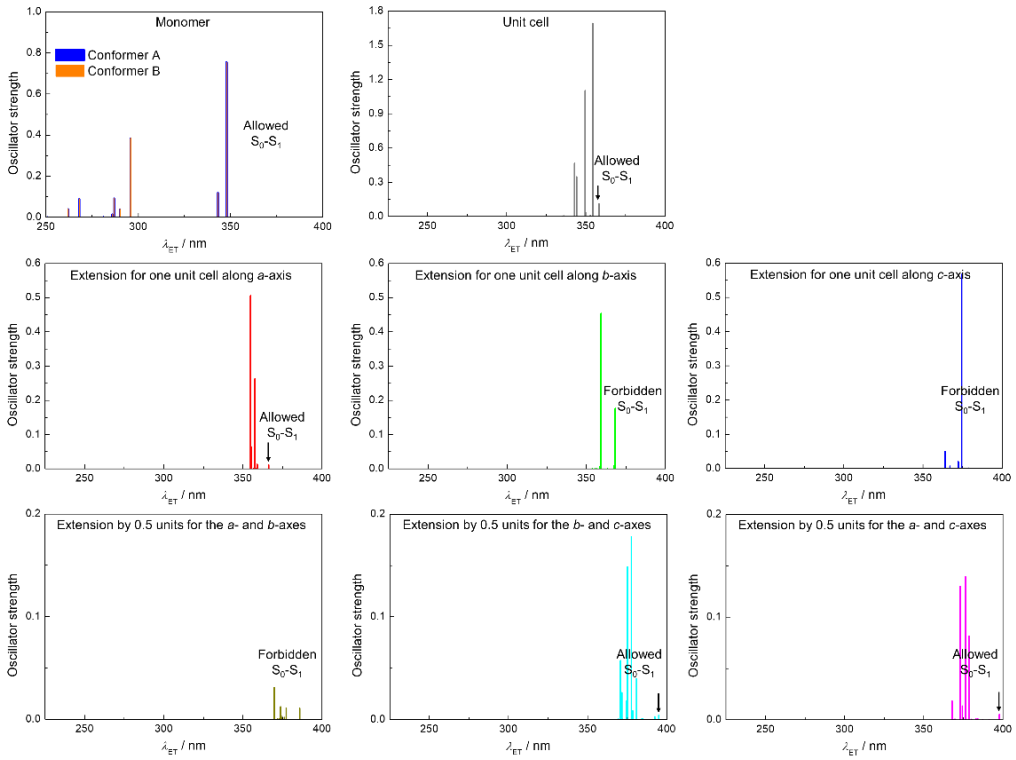

Fig. S17 Electronic transitions estimated for a single molecule, unit cell, and large supercell of **1ar** replaced by optimized structures based on the B3LYP/6-31G(d,p) level of theory using the TD-DFT method based on the B3LYP/6-31G(d,p) level of theory.

Table S8. Results of TD-DFT calculations with geometries of single molecule and unit cell of **1ar** replaced by optimized structures based on the B3LYP/6-31G(d,p) level of theory.

	Single molecule		
Excited states	Conformer A	Conformer B	Unit cell
1st	347.87 nm (3.56 eV) *f* = 0.7550 HOMO→LUMO: 0.70	347.87 nm (3.56 eV) *f* = 0.7549 HOMO→LUMO: 0.70	358.19 nm (3.46 eV) *f* = 0.0010 HOMO-1→LUMO: 0.49 HOMO→LUMO: 0.12 HOMO→LUMO+1: 0.46
2nd	343.07 nm (3.61 eV) *f* = 0.1187 HOMO-1→LUMO: 0.66 HOMO→LUMO+1: -0.22	343.06 nm (3.61 eV) *f* = 0.1186 HOMO-1→LUMO: 0.66 HOMO→LUMO+1: 0.22	358.15 nm (3.46 eV) *f* = 0.1097 HOMO-1→LUMO+1: 0.46 HOMO→LUMO: 0.46 HOMO→LUMO+1: -0.18
3rd	295.84 nm (4.19 eV) *f* = 0.3841 HOMO-2→LUMO: 0.13 HOMO-1→LUMO: 0.21 HOMO→LUMO+1: 0.65	295.84 nm (4.19 eV) *f* = 0.3842 HOMO-2→LUMO: -0.13 HOMO-1→LUMO: -0.21 HOMO→LUMO+1: 0.65	354.34 nm (3.50 eV) *f* = 1.6922 HOMO-1→LUMO+1: 0.14 HOMO-1→LUMO+2: 0.25 HOMO-1→LUMO+3: 0.40 HOMO→LUMO+2: 0.40 HOMO→LUMO+3: -0.25

4th	290.01 nm (4.28 eV) *f* = 0.0387 HOMO-3→LUMO: -0.10 HOMO-1→LUMO+1: 0.68	290.00 nm (4.28 eV) *f* = 0.0388 HOMO-3→LUMO: 0.10 HOMO-1→LUMO+1: 0.68	353.66 nm (3.51 eV) *f* = 0.0000 HOMO-7→LUMO+1: 0.11 HOMO-6→LUMO: -0.10 HOMO-3→LUMO: 0.24 HOMO-2→LUMO+1: 0.24 HOMO-1→LUMO+2: 0.35 HOMO-1→LUMO+3: -0.17 HOMO→LUMO+1: 0.17 HOMO→LUMO+2: 0.17 HOMO→LUMO+3: 0.35
5th	286.91 nm (4.32 eV) *f* = 0.0910 HOMO-3→LUMO+1: -0.13 HOMO-2→LUMO: 0.65 HOMO→LUMO+1: -0.11 HOMO→LUMO+5: 0.10	286.91 nm (4.32 eV) *f* = 0.0910 HOMO-3→LUMO+1: 0.13 HOMO-2→LUMO: 0.65 HOMO→LUMO+1: 0.11 HOMO→LUMO+5: -0.10	352.83 nm (3.51 eV) *f* = 0.0083 HOMO-1→LUMO: -0.34 HOMO-1→LUMO+1: -0.32 HOMO→LUMO: 0.48 HOMO→LUMO+1: 0.19
6th	285.92 nm (4.34 eV) *f* = 0.0142 HOMO-3→LUMO: 0.66 HOMO-2→LUMO+1: -0.13 HOMO-1→LUMO+1: 0.11 HOMO→LUMO+4: -0.11	285.92 nm (4.34 eV) *f* = 0.0141 HOMO-3→LUMO: 0.66 HOMO-2→LUMO+1: 0.13 HOMO-1→LUMO+1: -0.11 HOMO→LUMO+4: 0.11	352.82 nm (3.51 eV) *f* = 0.0037 HOMO-1→LUMO: -0.36 HOMO-1→LUMO+1: 0.38 HOMO→LUMO: -0.16 HOMO→LUMO+1: 0.43
7th	281.04 nm (4.41 eV) *f* = 0.0003 HOMO-7→LUMO+1: -0.16 HOMO-6→LUMO: 0.69	281.04 nm (4.41 eV) *f* = 0.0003 HOMO-7→LUMO+1: -0.16 HOMO-6→LUMO: 0.69	349.56 nm (3.55 eV) *f* = 1.1013 HOMO-3→LUMO: 0.25 HOMO-3→LUMO+1: 0.40 HOMO-2→LUMO: 0.40 HOMO-2→LUMO+1: -0.25
8th	268.27 nm (4.62 eV) *f* = 0.0000 HOMO-7→LUMO: 0.64 HOMO-6→LUMO+1: -0.29	268.27 nm (4.62 eV) *f* = 0.0000 HOMO-7→LUMO: 0.64 HOMO-6→LUMO+1: -0.29	349.32 nm (3.55 eV) *f* = 0.0000 HOMO-3→LUMO: 0.42 HOMO-2→LUMO+1: 0.42 HOMO-1→LUMO+2: -0.21 HOMO-1→LUMO+3: 0.10 HOMO→LUMO+2: -0.10 HOMO→LUMO+3: -0.21
9th	268.08 nm (4.62 eV) *f* = 0.0890 HOMO-4→LUMO: 0.63 HOMO-1→LUMO: 0.11 HOMO→LUMO+2: 0.25 HOMO→LUMO+5: 0.10	268.08 nm (4.62 eV) *f* = 0.0889 HOMO-4→LUMO: 0.63 HOMO-1→LUMO: -0.11 HOMO→LUMO+2: 0.25 HOMO→LUMO+5: 0.10	344.12 nm (3.60 eV) *f* = 0.3467 HOMO-7→LUMO: -0.45 HOMO-6→LUMO+1: 0.45 HOMO-3→LUMO+5: -0.14 HOMO-2→LUMO+4: -0.14
10th	262.01 nm (4.73 eV) *f* = 0.0395 HOMO-5→LUMO: 0.66 HOMO-1→LUMO+2: -0.17	262.00 nm (4.73 eV) *f* = 0.0395 HOMO-5→LUMO: 0.66 HOMO-1→LUMO+2: 0.17	343.91 nm (3.61 eV) *f* = 0.0000 HOMO-7→LUMO: -0.12 HOMO-7→LUMO+1: -0.34 HOMO-6→LUMO: 0.34 HOMO-6→LUMO+1: -0.12 HOMO-5→LUMO+2: 0.26 HOMO-5→LUMO+3: -0.11 HOMO-4→LUMO+2: 0.11 HOMO-4→LUMO+3: 0.26 HOMO-3→LUMO+4: -0.12 HOMO-2→LUMO+5: -0.12 HOMO-1→LUMO+7: -0.10 HOMO→LUMO+6: 0.10

11th	250.72 nm (4.95 eV) *f* = 0.0005 HOMO-3→LUMO: 0.20 HOMO-2→LUMO+1: 0.60 HOMO-1→LUMO+2: -0.19 HOMO→LUMO+3: -0.14 HOMO→LUMO+4: 0.15	250.72 nm (4.95 eV) *f* = 0.0005 HOMO-3→LUMO: -0.20 HOMO-2→LUMO+1: 0.60 HOMO-1→LUMO+2: -0.19 HOMO→LUMO+3: 0.14 HOMO→LUMO+4: 0.15	342.81 nm (3.62 eV) *f* = 0.4639 HOMO-5→LUMO+2: 0.26 HOMO-5→LUMO+3: 0.37 HOMO-4→LUMO+2: 0.37 HOMO-4→LUMO+3: -0.26 HOMO-1→LUMO+6: 0.15 HOMO→LUMO+7: -0.15
12th	249.79 nm (4.96 eV) *f* = 0.0015 HOMO-3→LUMO+1: 0.59 HOMO-2→LUMO: 0.20 HOMO-1→LUMO+4: -0.13 HOMO→LUMO+2: 0.21 HOMO→LUMO+5: -0.18	249.79 nm (4.96 eV) *f* = 0.0015 HOMO-3→LUMO+1: 0.59 HOMO-2→LUMO: -0.20 HOMO-1→LUMO+4: -0.13 HOMO→LUMO+2: 0.21 HOMO→LUMO+5: -0.18	342.16 nm (3.62 eV) *f* = 0.0000 HOMO-7→LUMO+1: 0.23 HOMO-6→LUMO: -0.23 HOMO-5→LUMO+2: 0.33 HOMO-5→LUMO+3: -0.13 HOMO-4→LUMO+2: 0.14 HOMO-4→LUMO+3: 0.33 HOMO-1→LUMO+2: -0.14 HOMO-1→LUMO+7: -0.11 HOMO→LUMO+3: -0.14 HOMO→LUMO+6: 0.11
13th	243.15 nm (5.10 eV) *f* = 0.0078 HOMO-4→LUMO: -0.24 HOMO-3→LUMO+1: -0.19 HOMO-1→LUMO+3: -0.27 HOMO→LUMO+2: 0.54	243.15 nm (5.10 eV) *f* = 0.0078 HOMO-4→LUMO: -0.24 HOMO-3→LUMO+1: -0.19 HOMO-1→LUMO+3: 0.27 HOMO→LUMO+2: 0.54	335.99 nm (3.69 eV) *f* = 0.0055 HOMO-5→LUMO: 0.26 HOMO-5→LUMO+1: 0.45 HOMO-4→LUMO: 0.45
14th	242.29 nm (5.12 eV) *f* = 0.1116 HOMO-9→LUMO: -0.11 HOMO-5→LUMO: 0.12 HOMO-4→LUMO+1: 0.26 HOMO-2→LUMO+1: 0.16 HOMO-1→LUMO+2: 0.49 HOMO→LUMO+3: 0.30 HOMO→LUMO+4: 0.18	242.29 nm (5.12 eV) *f* = 0.1115 HOMO-9→LUMO: 0.11 HOMO-5→LUMO: -0.12 HOMO-4→LUMO+1: -0.26 HOMO-2→LUMO+1: 0.16 HOMO-1→LUMO+2: 0.49 HOMO→LUMO+3: -0.30 HOMO→LUMO+4: 0.18	335.98 nm (3.69 eV) *f* = 0.0003 HOMO-5→LUMO: 0.43 HOMO-5→LUMO+1: -0.15 HOMO-4→LUMO+1: 0.51
15th	236.75 nm (5.24 eV) *f* = 0.0004 HOMO-7→LUMO: 0.29 HOMO-6→LUMO+1: 0.64	236.75 nm (5.24 eV) *f* = 0.0004 HOMO-7→LUMO: 0.29 HOMO-6→LUMO+1: 0.64	335.35 nm (3.70 eV) *f* = 0.0001 HOMO-5→LUMO: -0.37 HOMO-5→LUMO+1: -0.22 HOMO-4→LUMO: 0.46 HOMO-4→LUMO+1: 0.29

Table S9. Results of TD-DFT calculations with geometries of the large supercell extended by one unit cell along one axis of **1ar** replaced by optimized structures based on the B3LYP/6-31G(d,p) level of theory.

	Extension for one unit cell along one axis		
Excited states	*a*	*b*	*c*
1st	366.12 nm (3.39 eV) *f* = 0.0025 HOMO-1→LUMO: 0.65 HOMO→LUMO: 0.12 HOMO→LUMO+1: 0.23	388.41 nm (3.19 eV) *f* = 0.0000 HOMO-2→LUMO+2: 0.57 HOMO→LUMO+2: 0.39	393.15 nm (3.15 eV) *f* = 0.0000 HOMO→LUMO+2:0.48 HOMO→LUMO+4: 0.51

2nd	366.12 nm (3.39 eV) *f* = 0.0107 HOMO-1→LUMO: -0.22 HOMO-1→LUMO+1: -0.12 HOMO→LUMO+1: 0.65	368.10 nm (3.37 eV) *f* = 0.1762 HOMO-3→LUMO+2: 0.55 HOMO-2→LUMO+5: 0.23 HOMO-1→LUMO+2: -0.30 HOMO→LUMO+5: 0.13	378.66 nm (3.27 eV) *f* = 0.0010 HOMO→LUMO: 0.38 HOMO→LUMO+1: 0.59
3rd	359.44 nm (3.45 eV) *f* = 0.0000 HOMO-5→LUMO+2: 0.12 HOMO-4→LUMO+3: 0.13 HOMO-3→LUMO+3: -0.28 HOMO-3→LUMO+4: 0.29 HOMO-2→LUMO+2: 0.27 HOMO-2→LUMO+5: 0.29 HOMO-1→LUMO+6: -0.25 HOMO→LUMO+7: -0.24	367.42 nm (3.37 eV) *f* = 0.0000 HOMO-4→LUMO+2: 0.15 HOMO-2→LUMO+2: -0.39 HOMO→LUMO+2: 0.56	378.63 nm (3.27 eV) *f* = 0.0000 HOMO→LUMO: 0.59 HOMO→LUMO+1: -0.38
4th	358.87 nm (3.45 eV) *f* = 0.0128 HOMO-5→LUMO+3: 0.11 HOMO-4→LUMO+2: 0.12 HOMO-3→LUMO+2: -0.38 HOMO-3→LUMO+5: -0.19 HOMO-2→LUMO+3: 0.39 HOMO-2→LUMO+4: -0.19 HOMO-1→LUMO+6: -0.17 HOMO→LUMO+7: 0.18	367.38 nm (3.37 eV) *f* = 0.0091 HOMO-5→LUMO+2: 0.15 HOMO-3→LUMO+2: 0.23 HOMO-2→LUMO+3: 0.13 HOMO-1→LUMO+2: 0.61 HOMO→LUMO+5: 0.14	374.17 nm (3.31 eV) *f* = 0.5667 HOMO-1→LUMO: 0.14 HOMO-1→LUMO+2: 0.46 HOMO-1→LUMO+4: 0.47 HOMO→LUMO+7: -0.16
5th	358.25 nm (3.46 eV) *f* = 0.0001 HOMO-3→LUMO: 0.51 HOMO-2→LUMO: 0.48	363.23 nm (3.41 eV) *f* = 0.0002 HOMO-2→LUMO: -0.21 HOMO-1→LUMO: 0.49 HOMO→LUMO: 0.45	372.31 nm (3.33 eV) *f* = 0.0000 HOMO-2→LUMO: 0.33 HOMO-2→LUMO+1: -0.12 HOMO-1→LUMO: 0.25 HOMO-1→LUMO+1: 0.55
6th	358.25 nm (3.46 eV) *f* = 0.0001 HOMO-3→LUMO+1: -0.47 HOMO-2→LUMO+1: 0.51	363.22 nm (3.41 eV) *f* = 0.0002 HOMO-2→LUMO+1: 0.21 HOMO-1→LUMO+1: 0.49 HOMO→LUMO+1: -0.45	372.21 nm (3.33 eV) *f* = 0.0204 HOMO-2→LUMO: 0.12 HOMO-2→LUMO+1: 0.33 HOMO-1→LUMO: 0.54 HOMO-1→LUMO+1: -0.25 HOMO-1→LUMO+2: -0.11 HOMO-1→LUMO+4: -0.11
7th	358.01 nm (3.46 eV) *f* = 0.0000 HOMO-3→LUMO+3: -0.37 HOMO-3→LUMO+4: -0.13 HOMO-2→LUMO+2: 0.38 HOMO-2→LUMO+5: -0.13 HOMO-1→LUMO+6: 0.27 HOMO→LUMO+7: 0.27	359.15 nm (3.45 eV) *f* = 0.4539 HOMO11→LUMO+2: 0.31 HOMO-3→LUMO+2: -0.28 HOMO-2→LUMO+5: 0.40 HOMO-1→LUMO+7: -0.13 HOMO→LUMO+5: 0.28	369.31 nm (3.36 eV) *f* = 0.0000 HOMO-2→LUMO+2: 0.48 HOMO-2→LUMO+4: 0.49
8th	357.56 nm (3.47 eV) *f* = 0.2629 HOMO-3→LUMO+2: 0.28 HOMO-3→LUMO+5: -0.16 HOMO-2→LUMO+3: 0.29 HOMO-2→LUMO+4: -0.16 HOMO-1→LUMO+6: -0.33 HOMO-1→LUMO+7: -0.11 HOMO→LUMO+6: -0.11 HOMO→LUMO+7: 0.33	358.65 nm (3.46 eV) *f* = 0.0001 HOMO-2→LUMO: -0.13 HOMO-2→LUMO+1: -0.14 HOMO-2→LUMO+4: 0.50 HOMO→LUMO+4: 0.42	367.08 nm (3.38 eV) *f* = 0.0053 HOMO-4→LUMO: 0.64 HOMO-4→LUMO+1: 0.27

9th	356.78 nm (3.48 eV) *f* = 0.0002 HOMO-1→LUMO+3: 0.20 HOMO→LUMO+2: 0.50 HOMO→LUMO+3: -0.45	358.64 nm (3.46 eV) *f* = 0.0075 HOMO-2→LUMO: 0.14 HOMO-2→LUMO+1: -0.12 HOMO-2→LUMO+3: 0.50 HOMO→LUMO+3: 0.41	367.07 nm (3.38 eV) *f* = 0.0066 HOMO-3→LUMO: -0.27 HOMO-3→LUMO+1: 0.64
10th	356.76 nm (3.48 eV) *f* = 0.0006 HOMO-1→LUMO+2: 0.48 HOMO-1→LUMO+3: 0.46 HOMO→LUMO+3: 0.20	356.94 nm (3.47 eV) *f* = 0.0000 HOMO-8→LUMO+2: 0.64 HOMO-4→LUMO+2: 0.16 HOMO→LUMO+2: -0.11	363.90 nm (3.41 eV) *f* = 0.0498 HOMO-7→LUMO+2: -0.13 HOMO-5→LUMO+2: 0.42 HOMO-5→LUMO+4: 0.46 HOMO→LUMO+7: -0.25
11th	355.44 nm (3.49 eV) *f* = 0.0000 HOMO-5→LUMO+2: 0.34 HOMO-4→LUMO+3: 0.34 HOMO-3→LUMO+4: 0.16 HOMO-2→LUMO+2: -0.19 HOMO-2→LUMO+5: 0.17 HOMO-1→LUMO+6: 0.23 HOMO→LUMO+7: 0.23	356.52 nm (3.48 eV) *f* = 0.0001 HOMO-2→LUMO: 0.55 HOMO-2→LUMO+1: -0.11 HOMO-2→LUMO+3: -0.14 HOMO→LUMO: 0.34 HOMO→LUMO+3: -0.12	362.03 nm (3.42 eV) *f* = 0.0000 HOMO-5→LUMO: -0.16 HOMO-2→LUMO: 0.36 HOMO-2→LUMO+1: 0.47 HOMO-1→LUMO: -0.35
12th	354.93 nm (3.49 eV) *f* = 0.0645 HOMO-3→LUMO+2: 0.45 HOMO-3→LUMO+3: -0.14 HOMO-2→LUMO+2: -0.17 HOMO-2→LUMO+3: 0.48	356.51 nm (3.48 eV) *f* = 0.0001 HOMO-2→LUMO: 0.11 HOMO-2→LUMO+1: 0.55 HOMO-2→LUMO+3: 0.10 HOMO-2→LUMO+4: 0.14 HOMO→LUMO+1: 0.34 HOMO→LUMO+4: 0.12	362.01 nm (3.42 eV) *f* = 0.0000 HOMO-5→LUMO+1: -0.16 HOMO-2→LUMO: 0.47 HOMO-2→LUMO+1: -0.36 HOMO-1→LUMO+1: -0.35
13th	354.92 nm (3.49 eV) *f* = 0.0071 HOMO-3→LUMO+2: 0.15 HOMO-3→LUMO+3: 0.49 HOMO-2→LUMO+2: 0.44 HOMO-2→LUMO+3: 0.14	355.68 nm (3.49 eV) *f* = 0.0002 HOMO-10→LUMO: -0.11 HOMO-9→LUMO+1: -0.11 HOMO-7→LUMO+4: -0.37 HOMO-6: LUMO+3: 0.37 HOMO-2→LUMO+7: -0.13 HOMO-1→LUMO+6: 0.27 HOMO→LUMO+7: 0.24	360.28 nm (3.44 eV) *f* = 0.0008 HOMO-2→LUMO+3: -0.14 HOMO-1→LUMO+2: -0.19 HOMO-1→LUMO+4: 0.18 HOMO→LUMO+3: 0.63
14th	354.84 nm (3.49 eV) *f* = 0.5060 HOMO-5→LUMO+3: 0.11 HOMO-4→LUMO+2: 0.11 HOMO-3→LUMO+5: -0.16 HOMO-2→LUMO+4: -0.16 HOMO-1→LUMO+2: -0.32 HOMO-1→LUMO+3: 0.20 HOMO-1→LUMO+6: 0.12 HOMO→LUMO+2: 0.27 HOMO→LUMO+3: 0.39 HOMO→LUMO+7: -0.12	353.61 nm (3.51 eV) *f* = 0.0000 HOMO-2→LUMO+3: 0.20 HOMO-2→LUMO+4: -0.23 HOMO-1→LUMO: 0.13 HOMO-1→LUMO+3: 0.38 HOMO-1→LUMO+4: -0.32 HOMO→LUMO: -0.11 HOMO→LUMO+3: -0.23 HOMO→LUMO+4: 0.26	360.25 nm (3.44 eV) *f* = 0.0000 HOMO-2→LUMO+4: 0.10 HOMO-1→LUMO+3: -0.27 HOMO→LUMO+2: 0.46 HOMO→LUMO+4: -0.43
15th	354.79 nm (3.49 eV) *f* = 0.0104 HOMO-1→LUMO+2: -0.31 HOMO-1→LUMO+3: 0.42 HOMO→LUMO+2: -0.38 HOMO→LUMO+3: -0.25	353.61 nm (3.51 eV) *f* = 0.0001 HOMO-2→LUMO+3: -0.23 HOMO-2→LUMO+4: -0.19 HOMO-1→LUMO+1: -0.13 HOMO-1→LUMO+3: 0.32 HOMO-1→LUMO+4: 0.38 HOMO→LUMO+1: -0.10 HOMO→LUMO+3: 0.27 HOMO→LUMO+4: 0.22	354.65 nm (3.50 eV) *f* = 0.0001 HOMO-2→LUMO+2: 0.21 HOMO-2→LUMO+4: -0.22 HOMO-1→LUMO+3: 0.55 HOMO→LUMO+2: 0.22 HOMO→LUMO+4: -0.21

Table S10. Results of TD-DFT calculations with geometries of the large supercell extended by 0.5 unit cells for two axes of **1ar** replaced by optimized structures based on the B3LYP/6-31G(d,p) level of theory.

	Extension by 0.5 units for two axes		
Excited states	*a* and *b*	*b* and *c*	*a* and *c*
1st	399.21 nm (3.11 eV) *f* = 0.0000 HOMO→LUMO+3: 0.12 HOMO→LUMO+4: -0.12 HOMO→LUMO+5: -0.46 HOMO→LUMO+6: 0.49	394.99 nm (3.14 eV) *f* = 0.0042 HOMO→LUMO: -0.14 HOMO→LUMO+2: --0.17 HOMO→LUMO+5: 0.62 HOMO→LUMO+6: 0.21	397.72 nm (3.12 eV) *f* = 0.0051 HOMO-2→LUMO+4: -0.10 HOMO→LUMO+4: 0.69
2nd	385.79 nm (3.21 eV) *f* = 0.0107 HOMO-1→LUMO+3: 0.13 HOMO-1→LUMO+4: -0.11 HOMO-1→LUMO+5: -0.41 HOMO-1→LUMO+6: 0.45 HOMO-1→LUMO-7: -0.20 HOMO-1→LUMO+8: 0.17 HOMO→LUMO+7: -0.13	392.93 nm (3.16 eV) *f* = 0.0005 HOMO→LUMO: 0.69 HOMO→LUMO+5: 0.12	391.25 nm (3.17 eV) *f* = 0.0002 HOMO→LUMO: 0.70
3rd	382.31 nm (3.24 eV) *f* = 0.0000 HOMO→LUMO: 0.71	392.29 nm (3.16 eV) *f* = 0.0028 HOMO-3→LUMO+2: 0.52 HOMO-2→LUMO+2: -0.30 HOMO-1→LUMO+2: 0.32	387.18 nm (3.20 eV) *f* = 0.0002 HOMO→LUMO+1: 0.70
4th	380.96 nm (3.25 eV) *f* = 0.0000 HOMO-1→LUMO+2: 0.12 HOMO→LUMO+1: -0.40 HOMO→LUMO+2: 0.57	392.12 nm (3.16 eV) *f* = 0.0002 HOMO→LUMO+1: 0.69	384.01 nm (3.23 eV) *f* = 0.0010 HOMO-3→LUMO: -0.17 HOMO-1→LUMO: 0.68
5th	379.46 nm (3.27 eV) *f* = 0.0000 HOMO→LUMO+1: 0.58 HOMO→LUMO+2: 0.40	384.66 nm (3.22 eV) *f* = 0.0008 HOMO-3→LUMO: 0.17 HOMO-2→LUMO: 0.67 HOMO-1→LUMO: 0.11	383.03 nm (3.24 eV) *f* = 0.0009 HOMO→LUMO+2: 0.70
6th	377.26 nm (3.29 eV) *f* = 0.0108 HOMO→LUMO+3: 0.16 HOMO→LUMO+7: 0.55 HOMO→LUMO+8: 0.15	384.21 nm (3.23 eV) *f* = 0.0008 HOMO-3→LUMO+1: -0.15 HOMO-1→LUMO+1: 0.68	380.09 nm (3.26 eV) *f* = 0.0004 HOMO-3→LUMO+1: -0.14 HOMO-1→LUMO+1: 0.69
7th	376.16 nm (3.30 eV) *f* = 0.0017 HOMO-2→LUMO+3: 0.16 HOMO-1→LUMO+3: -0.41 HOMO→LUMO+3: 0.44 HOMO→LUMO+7: -0.29	380.83 nm (3.26 eV) *f* = 0.0395 HOMO-4→LUMO+2: 0.12 HOMO-2→LUMO+2: -0.14 HOMO-1→LUMO+2: -0.12 HOMO→LUMO+2: 0.63 HOMO→LUMO+5: 0.12 HOMO→LUMO+6: 0.13	378.50 nm (3.28 eV) *f* = 0.0814 HOMO-2→LUMO+4: -0.17 HOMO-1→LUMO+4: -0.23 HOMO→LUMO+7: 0.62
8th	374.52 nm (3.31 eV) *f* = 0.0005 HOMO-2→LUMO+2: 0.20 HOMO-1→LUMO+1: -0.39 HOMO-1→LUMO+2: 0.53 HOMO→LUMO+2: -0.13	378.52 nm (3.28 eV) *f* = 0.0084 HOMO-2→LUMO: -0.12 HOMO-1→LUMO: 0.68	376.70 nm (3.29 eV) *f* = 0.0011 HOMO-5→LUMO: 0.70
9th	374.15 nm (3.31 eV)	377.58 nm (3.28 eV)	376.29 nm (3.29 eV)

	f = 0.0015 HOMO-2→LUMO+5: -0.18 HOMO-2→LUMO+6: 0.19 HOMO-1→LUMO: 0.44 HOMO-1→LUMO+3: 0.34 HOMO→LUMO+3: 0.29	*f* = 0.1781 HOMO-6→LUMO+2: 0.15 HOMO-4→LUMO+2: -0.14 HOMO-3→LUMO+2: -0.32 HOMO-3→LUMO+5: 0.13 HOMO-2→LUMO+2: -0.21 HOMO-2→LUMO+5: 0.18 HOMO-1→LUMO: -0.13 HOMO-1→LUMO+2: 0.33 HOMO-1→LUMO+5: -0.30	*f* = 0.1392 HOMO-1→LUMO+4: 0.64 HOMO→LUMO+7: 0.22
10th	373.96 nm (3.32 eV) *f* = 0.0037 HOMO-2→LUMO+5: 0.24 HOMO-2→LUMO+6: -0.26 HOMO-2→LUMO+7: 0.11 HOMO-1→LUMO: 0.53 HOMO-1→LUMO+3: -0.21 HOMO→LUMO+3: -0.12	375.15 nm (3.30 eV) *f* = 0.1486 HOMO-2→LUMO+1: 0.28 HOMO-2→LUMO+2: 0.34 HOMO-2→LUMO+5: -0.33 HOMO-1→LUMO+2: 0.17 HOMO-1→LUMO+5: -0.29 HOMO→LUMO+2: 0.16	374.30 nm (3.31 eV) *f* = 0.0135 HOMO-6→LUMO: -0.13 HOMO-2→LUMO: 0.66 HOMO-2→LUMO+4: 0.15
11th	373.73 nm (3.32 eV) *f* = 0.0122 HOMO-2→LUMO+3: -0.17 HOMO-2→LUMO+5: 0.28 HOMO-2→LUMO+6: -0.30 HOMO-2→LUMO+7: 0.13 HOMO-1→LUMO: -0.18 HOMO-1→LUMO+3: 0.31 HOMO→LUMO+3: 0.27 HOMO→LUMO+7: -0.16 HOMO→LUMO+8: -0.11	374.73 nm (3.31 eV) *f* = 0.0183 HOMO-4→LUMO+1: 0.14 HOMO-2→LUMO+1: 0.62 HOMO-2→LUMO+2: -0.18 HOMO-2→LUMO+5: 0.13 HOMO-1→LUMO+5: 0.12	373.08 nm (3.32 eV) *f* = 0.1301 HOMO-2→LUMO: -0.17 HOMO-2→LUMO+4: 0.61 HOMO-2→LUMO+8: -0.11 HOMO→LUMO+7: 0.17 HOMO→LUMO+8: 0.10
12th	373.12 nm (3.32 eV) *f* = 0.0003 HOMO-2→LUMO+2: 0.11 HOMO-1→LUMO+1: 0.59 HOMO-1→LUMO+2: 0.37	372.04 nm (3.33 eV) *f* = 0.0003 HOMO-4→LUMO: -0.39 HOMO-3→LUMO: 0.55 HOMO-2→LUMO: -0.18	369.91 nm (3.35 eV) *f* = 0.0003 HOMO-3→LUMO+2: 0.42 HOMO-1→LUMO+2: 0.55
13th	371.77 nm (3.34 eV) *f* = 0.0007 HOMO→LUMO+5: 0.51 HOMO→LUMO+6: 0.47	371.56 nm (3.34 eV) *f* = 0.0261 HOMO-6→LUMO+2: -0.21 HOMO-4→LUMO+2: 0.11 HOMO-3→LUMO+2: 0.15 HOMO-3→LUMO+6: 0.23 HOMO-2→LUMO+2: 0.21 HOMO-2→LUMO+5: 0.43 HOMO-1→LUMO+2: -0.12 HOMO-1→LUMO+5: -0.30	369.32 nm (3.36 eV) *f* = 0.0005 HOMO-3→LUMO+1: 0.21 HOMO-1→LUMO+1: 0.67
14th	369.78 nm (3.35 eV) *f* = 0.0092 HOMO-3→LUMO+5: -0.16 HOMO-3→LUMO+6: 0.18 HOMO→LUMO+4: 0.60 HOMO→LUMO+8: -0.18	370.66 nm (3.35 eV) *f* = 0.0574 HOMO-6→LUMO+2: 0.11 HOMO-4→LUMO+2: -0.11 HOMO-3→LUMO+6: -0.11 HOMO-2→LUMO+2: 0.35 HOMO-2→LUMO+5: 0.21 HOMO-2→LUMO+6: 0.17 HOMO-1→LUMO+2: 0.29 HOMO-1→LUMO+5: 0.33 HOMO→LUMO+7: 0.11	368.77 nm (3.36 eV) *f* = 0.0001 HOMO-2→LUMO+2: 0.68 HOMO-1→LUMO+2: 0.14
15th	369.61 nm (3.35 eV) *f* = 0.0307 HOMO-3→LUMO+5: 0.31 HOMO-3→LUMO+6: -0.34 HOMO→LUMO+4: 0.34 HOMO→LUMO+8: 0.33	369.32 nm (3.36 eV) *f* = 0.0003 HOMO-4→LUMO: 0.58 HOMO-3→LUMO: 0.40	367.85 nm (3.37 eV) *f* = 0.0181 HOMO-3→LUMO: 0.17 HOMO-3→LUMO+4: 0.64

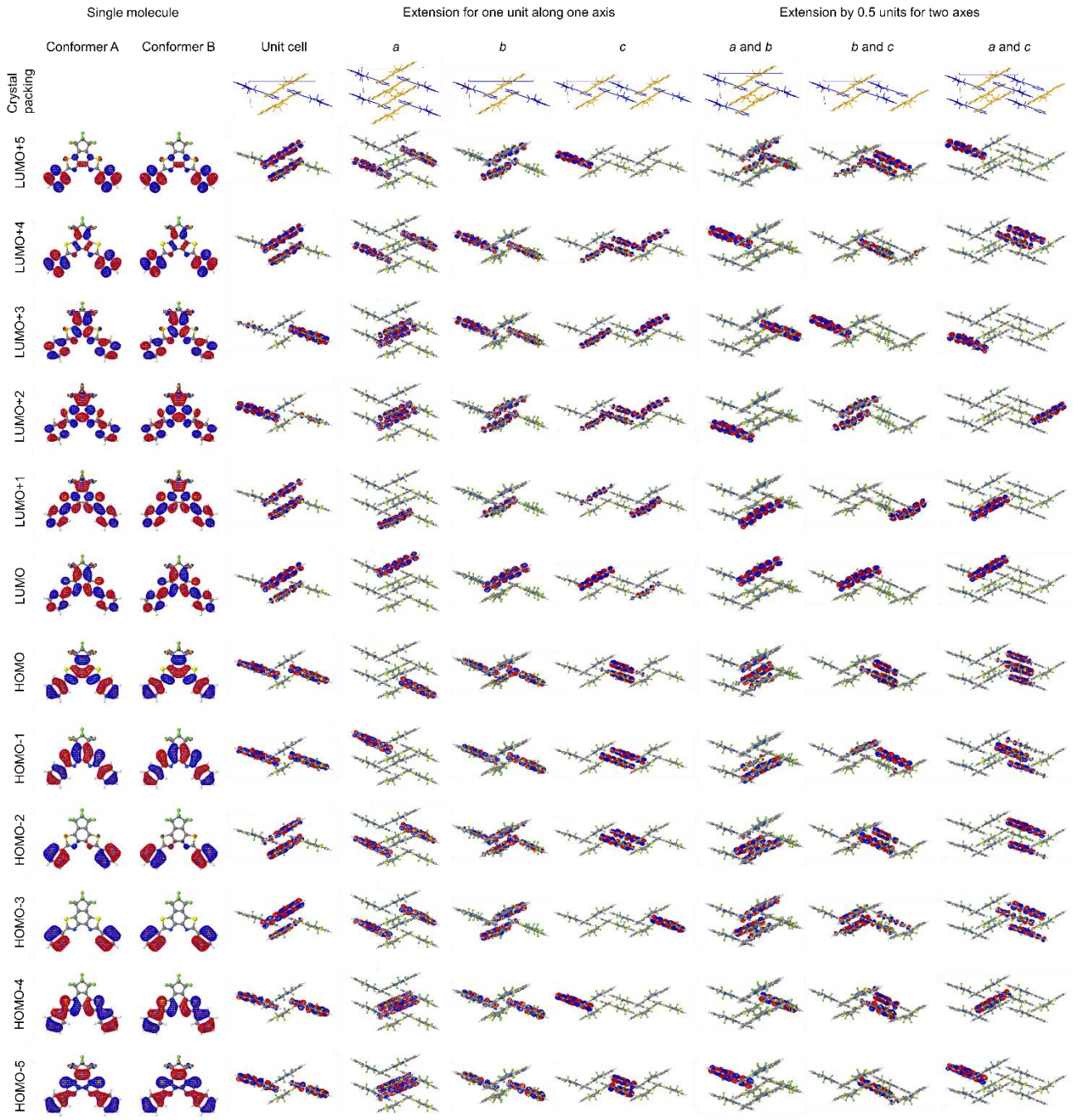

Fig. S18 Kohn-Sham molecular orbitals estimated for a single molecule, unit cell, and large supercell of **1ar** with geometries replaced by optimized structures based on the B3LYP/6-31G(d,p) level of theory.

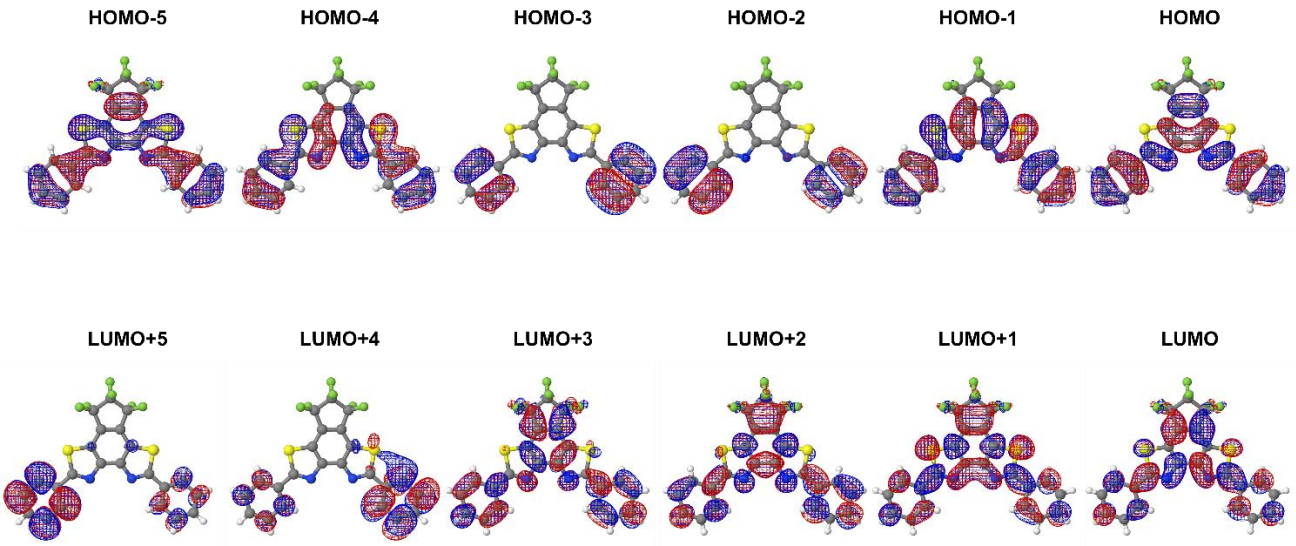

Fig. S19 Molecular orbitals of conformer A of **1ar** obtained by RHF/6-31G(d) calculation.

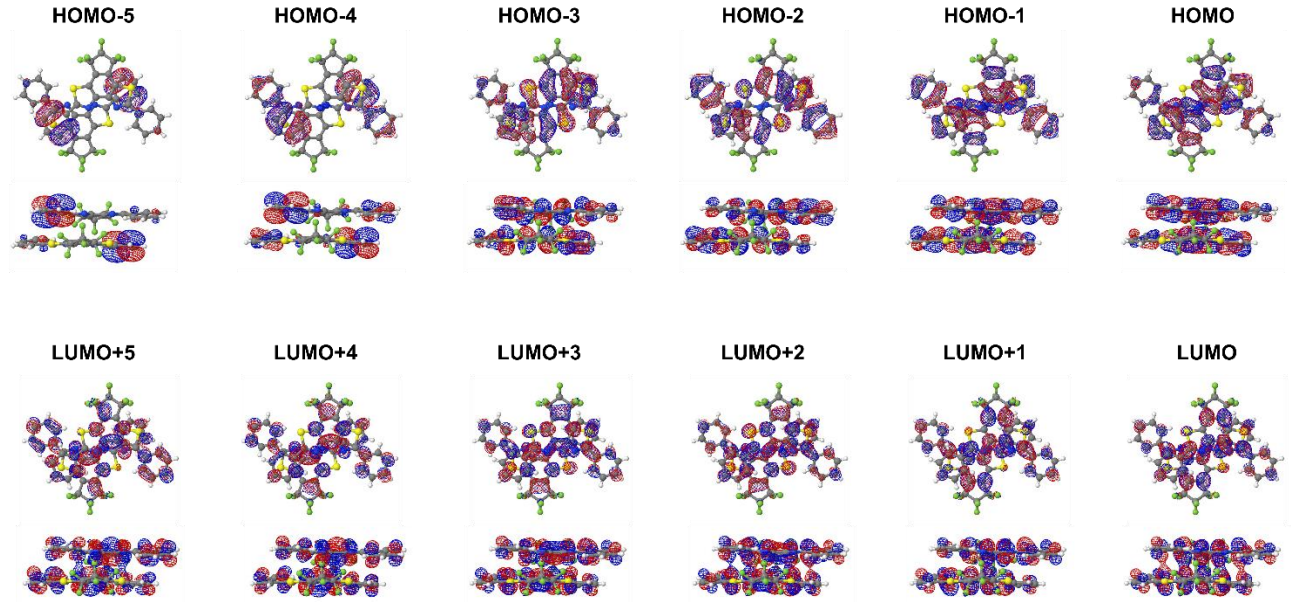

Fig. S20 Molecular orbitals of a dimer of conformer A of **1ar** shown in the left panel in Fig. 4b obtained by RHF/6-31G(d) calculation.

Table S11. Results of TDDFT/6-31G(d,p) calculations of dimer of **1ar** with geometries of crystal structure obtained by X-ray crystallographic analysis.

Excited states	Dimer of conformer A: Type 1	Dimer of conformer A: Type 2	Dimer of conformer B: Type 3	Dimer of conformer B: Type 4
1st	373.97 nm (3.32 eV) *f* = 0.0000 HOMO→LUMO: 0.70	360.04 nm (3.44 eV) *f* = 0.0000 HOMO→LUMO: 0.69	379.54 nm (3.27 eV) *f* = 0.0000 HOMO→LUMO: 0.70	357.80 nm (3.47 eV) *f* = 0.0000 HOMO-1→LUMO+1: 0.27 HOMO→LUMO: 0.65
2nd	353.99 nm (3.50 eV) *f* = 0.1663 HOMO-3→LUMO: 0.31 HOMO-1→LUMO: 0.55 HOMO→LUMO+1: -0.30	352.24 nm (3.52 eV) *f* = 0.0419 HOMO-3→LUMO: -0.13 HOMO-1→LUMO: -0.35 HOMO→LUMO+1: 0.59	357.31 nm (3.47 eV) *f* = 0.0244 HOMO-3→LUMO: 0.22 HOMO-1→LUMO: -0.43 HOMO→LUMO+1: 0.51	355.81 nm (3.48 eV) *f* = 0.0166 HOMO-1→LUMO: 0.51 HOMO→LUMO+1: 0.48
3rd	352.03 nm (3.52 eV) *f* = 0.0000 HOMO-2→LUMO: 0.69	342.53 nm (3.62 eV) *f* = 0.0000 HOMO-3→LUMO+1: 0.17 HOMO-1→LUMO+1: 0.67	349.69 nm (3.55 eV) *f* = 0.4119 HOMO-3→LUMO: 0.34 HOMO-1→LUMO: 0.52 HOMO→LUMO+1: 0.30	351.63 nm (3.53 eV) *f* = 0.0000 HOMO-3→LUMO+1: 0.11 HOMO-2→LUMO: -0.24 HOMO-1→LUMO+1: 0.60 HOMO→LUMO: -0.25
4th	351.25 nm (3.53 eV) *f* = 0.1156 HOMO-3→LUMO: 0.59 HOMO-1→LUMO: -0.35	341.38 nm (3.63 eV) *f* = 1.0311 HOMO-1→LUMO: 0.61 HOMO→LUMO+1: 0.34	344.62 nm (3.60 eV) *f* = 0.0000 HOMO-2→LUMO: 0.68 HOMO-1→LUMO+3: 0.11	347.14 nm (3.57 eV) *f* = 0.0000 HOMO-2→LUMO: 0.65 HOMO-1→LUMO+1: 0.22 HOMO→LUMO+1: -0.11
5th	333.32 nm (3.72 eV) *f* = 0.4533 HOMO-3→LUMO: 0.14 HOMO-2→LUMO+1: -0.24 HOMO-1→LUMO: 0.21 HOMO→LUMO+1: 0.58 HOMO→LUMO+2: 0.14	333.72 nm (3.72 eV) *f* = 0.1349 HOMO-3→LUMO: 0.56 HOMO-2→LUMO+1: -0.31 HOMO-1→LUMO+3: 0.11 HOMO→LUMO+2: 0.21	341.15 nm (3.63 eV) *f* = 0.6329 HOMO-3→LUMO: 0.53 HOMO-1→LUMO: -0.18 HOMO→LUMO+1: -0.36 HOMO→LUMO+2: 0.17	344.96 nm (3.59 eV) *f* = 0.1134 HOMO-3→LUMO: -0.28 HOMO-2→LUMO+1: 0.46 HOMO-1→LUMO: 0.30 HOMO→LUMO+1: -0.32
6th	329.35 nm (3.79 eV) *f* = 0.0000 HOMO-1→LUMO+1: 0.69	333.03 nm (3.72 eV) *f* = 0.0000 HOMO-3→LUMO+1: -0.27 HOMO-2→LUMO: 0.62 HOMO→LUMO+3: -0.12	332.84 nm (3.73 eV) *f* = 0.0000 HOMO-3→LUMO+1: -0.22 HOMO-1→LUMO+1: 0.65	336.94 nm (3.68 eV) *f* = 0.1595 HOMO-3→LUMO: 0.61 HOMO-1→LUMO: 0.12 HOMO-1→LUMO+3: 0.14 HOMO→LUMO+1: -0.21 HOMO→LUMO+2: 0.11

Table S12. Results of CIS/3-21G and CIS(D)/3-21G calculations of dimer of **1ar** with geometries of crystal structure obtained by X-ray crystallographic analysis.

Excited states	Dimer of conformer A: Type 1	Dimer of conformer A: Type 2	Dimer of conformer B: Type 3	Dimer of conformer B: Type 4
1st	CIS 266.25 nm (4.66 eV) *f* = 0.0000 HOMO-3→LUMO+2: 0.17 HOMO-2→LUMO+3: 0.15 HOMO-1→LUMO+1: -0.34 HOMO→LUMO: 0.50 CIS(D) 267.82 nm (4.63 eV)	CIS 262.47 nm (4.72 eV) *f* = 0.0000 HOMO-3→LUMO+2: 0.18 HOMO-2→LUMO+3: -0.16 HOMO-1→LUMO+1: -0.40 HOMO→LUMO: 0.43 HOMO→LUMO+3: 0.12 CIS(D) 262.37 nm (4.73 eV)	CIS 269.14 nm (4.61 eV) *f* = 0.0000 HOMO-3→LUMO+2: 0.18 HOMO-2→LUMO+3: 0.16 HOMO-1→LUMO+1: -0.31 HOMO→LUMO: 0.52 HOMO→LUMO+3: -0.11 CIS(D) 271.10 nm (4.57 eV)	CIS 266.68 nm (4.65 eV) *f* = 0.0000 HOMO-3→LUMO+2: -0.17 HOMO-2→LUMO+3: -0.16 HOMO-1→LUMO+1: 0.42 HOMO→LUMO: 0.44 CIS(D) 266.49 nm (4.65 eV)
2nd	CIS 256.28 nm (4.84 eV) *f* = 1.6763 HOMO-3→LUMO+3: -0.19 HOMO-2→LUMO+1: 0.12 HOMO-2→LUMO+2: -0.22 HOMO-1→LUMO: 0.45 HOMO→LUMO+1: -0.36 CIS(D) 254.84 nm (4.87 eV)	CIS 259.25 nm (4.78 eV) *f* = 1.9339 HOMO-3→LUMO+3: -0.18 HOMO-2→LUMO+1: 0.17 HOMO-2→LUMO+2: 0.20 HOMO-1→LUMO: 0.42 HOMO→LUMO+1: 0.39 CIS(D) 257.14 nm (4.82 eV)	CIS 260.59 nm (4.76 eV) *f* = 1.9346 HOMO-3→LUMO+3: 0.17 HOMO-2→LUMO+1: -0.19 HOMO-2→LUMO+2: 0.18 HOMO-1→LUMO: 0.43 HOMO→LUMO+1: -0.36 CIS(D) 258.53 nm (4.80 eV)	CIS 257.86 nm (4.81 eV) *f* = 1.6743 HOMO-3→LUMO+3: 0.19 HOMO-2→LUMO+2: 0.22 HOMO-1→LUMO: 0.40 HOMO→LUMO+1: 0.42 CIS(D) 256.08 nm (4.84 eV)
3rd	CIS 239.81 nm (5.17 eV) *f* = 0.0000 HOMO-3→LUMO+1: 0.34 HOMO-2→LUMO: 0.49 HOMO-1→LUMO+1: 0.12 HOMO-1→LUMO+4: 0.12 HOMO→LUMO: 0.10 HOMO→LUMO+5: -0.12 CIS(D) 283.06 nm (4.38 eV)	CIS 238.36 nm (5.20 eV) *f* = 0.0000 HOMO-3→LUMO+1: 0.37 HOMO-2→LUMO: 0.44 HOMO-1→LUMO+1: 0.12 HOMO-1→LUMO+2: 0.10 HOMO-1→LUMO+5: 0.11 HOMO→LUMO: -0.15 HOMO→LUMO+4: 0.14 CIS(D) 275.02 nm (4.51 eV)	CIS 241.52 nm (5.13 eV) *f* = 0.0000 HOMO-3→LUMO+1: -0.31 HOMO-2→LUMO: 0.46 HOMO-1→LUMO+1: -0.24 HOMO-1→LUMO+4: -0.11 HOMO→LUMO: -0.12 HOMO→LUMO+5: -0.12 CIS(D) 275.87 nm (4.49 eV)	CIS 239.50 nm (5.18 eV) *f* = 0.0000 HOMO-10→LUMO+2: 0.11 HOMO-3→LUMO: -0.41 HOMO-2→LUMO+1: 0.45 HOMO-1→LUMO+4: 0.13 HOMO→LUMO+5: 0.12 CIS(D) 282.02 nm (4.40 eV)
4th	CIS 234.85 nm (5.28 eV) *f* = 0.6499 HOMO-3→LUMO: 0.48 HOMO-2→LUMO+1: 0.36 HOMO-1→LUMO+5: 0.12 HOMO→LUMO+4: -0.15 CIS(D) 287.54 nm (4.31 eV)	CIS 233.17 nm (5.31 eV) *f* = 0.6621 HOMO-11→LUMO+2: -0.10 HOMO-10→LUMO+3: -0.10 HOMO-8→LUMO: 0.12 HOMO-3→LUMO: 0.39 HOMO-2→LUMO+1: 0.40 HOMO-1→LUMO+4: 0.14 HOMO→LUMO+1: -0.20 HOMO→LUMO+5: 0.14 CIS(D) 286.17 nm (4.33 eV)	CIS 235.28 nm (5.27 eV) *f* = 0.6728 HOMO-11→LUMO+2: -0.10 HOMO-3→LUMO: 0.44 HOMO-2→LUMO+1: -0.35 HOMO-1→LUMO: 0.12 HOMO-1→LUMO+5: -0.13 HOMO→LUMO+1: 0.18 HOMO→LUMO+4: -0.14 CIS(D) 286.18 nm (4.33 eV)	CIS 235.33 nm (5.27 eV) *f* = 0.7409 HOMO-10→LUMO+3: 0.48 HOMO-3→LUMO+1: 0.48 HOMO-2→LUMO: 0.36 HOMO-1→LUMO+5: 0.12 HOMO→LUMO+4: -0.15 CIS(D) 282.91 nm (4.38 eV)

5th	CIS 219.20 nm (5.66 eV) *f* = 0.6226 HOMO-9→LUMO+1: -0.11 HOMO-8→LUMO: -0.22 HOMO-4→LUMO: -0.13 HOMO-2→LUMO+6: 0.11 HOMO-1→LUMO+3: -0.34 HOMO→LUMO+2: 0.42 CIS(D) 231.75 nm (5.35 eV)	CIS 221.16 nm (5.61 eV) *f* = 0.0000 HOMO-9→LUMO: -0.17 HOMO-8→LUMO+1: -0.18 HOMO-5→LUMO+1: -0.11 HOMO-3→LUMO+6: -0.10 HOMO-2→LUMO+3: -0.14 HOMO-2→LUMO+7: 0.12 HOMO-1→LUMO+2: 0.40 HOMO→LUMO+3: -0.34 CIS(D) 245.10 nm (5.06 eV)	CIS 221.25 nm (5.60 eV) *f* = 0.0000 HOMO-9→LUMO: 0.20 HOMO-8→LUMO+1: 0.17 HOMO-3→LUMO+1: 0.10 HOMO-3→LUMO+6: 0.11 HOMO-2→LUMO+3: 0.15 HOMO-2→LUMO+7: -0.10 HOMO-1→LUMO+2: 0.35 HOMO→LUMO+3: 0.36 CIS(D) 248.05 nm (5.00 eV)	CIS 219.68 nm (5.64 eV) *f* = 0.0001 HOMO-9→LUMO: 0.16 HOMO-8→LUMO+1: -0.16 HOMO-6→LUMO: -0.11 HOMO-3→LUMO+7: -0.10 HOMO-2→LUMO+6: -0.11 HOMO-1→LUMO+3: -0.35 HOMO→LUMO+2: 0.40 CIS(D) 242.38 nm (5.12 eV)
6th	CIS 218.30 nm (5.68 eV) *f* = 0.0000 HOMO-10→LUMO: 0.10 HOMO-9→LUMO: 0.15 HOMO-8→LUMO+1: 0.14 HOMO-4→LUMO+1: 0.12 HOMO-3→LUMO+6: -0.10 HOMO-2→LUMO+3: 0.10 HOMO-1→LUMO+2: 0.39 HOMO→LUMO+3: -0.36 CIS(D) 239.95 nm (5.17 eV)	CIS 217.45 nm (5.70 eV) *f* = 0.7742 HOMO-9→LUMO+1: -0.14 HOMO-8→LUMO: -0.17 HOMO-5→LUMO: -0.11 HOMO-3→LUMO+7: 0.10 HOMO-2→LUMO+2: 0.10 HOMO-2→LUMO+6: -0.11 HOMO-1→LUMO+3: -0.37 HOMO→LUMO+2: 0.40 CIS(D) 227.78 nm (5.44 eV)	CIS 219.57 nm (5.65 eV) *f* = 0.6646 HOMO-9→LUMO+1: -0.15 HOMO-8→LUMO+1: -0.19 HOMO-3→LUMO+7: -0.11 HOMO-2→LUMO+6: 0.11 HOMO-1→LUMO+3: 0.34 HOMO→LUMO+2: 0.43 CIS(D) 232.33 nm (5.34 eV)	CIS 219.28 nm (5.65 eV) *f* = 0.5134 HOMO-9→LUMO+1: 0.17 HOMO-8→LUMO: -0.18 HOMO-6→LUMO+1: -0.12 HOMO-3→LUMO+6: 0.12 HOMO-2→LUMO+7: 0.11 HOMO-1→LUMO+2: 0.41 HOMO→LUMO+3: -0.37 CIS(D) 234.77 nm (5.28 eV)

Table S13. Results of CIS/3-21G and CIS(D)/3-21G calculations of monomer of **1ar** with geometries of crystal structure obtained by X-ray crystallographic analysis.

Excited States	Conformer A	Conformer B
1st	CIS 258.52 nm (4.80 eV) *f* = 1.0516 HOMO-4→LUMO+2: -0.11 HOMO-1→LUMO+1: -0.28 HOMO→LUMO: 0.60 CIS(D) 255.20 nm (4.86 eV)	CIS 260.71 nm (4.76 eV) *f* = 1.0786 HOMO-4→LUMO+2: -0.10 HOMO-1→LUMO+1: -0.28 HOMO→LUMO: 0.60 CIS(D) 257.31 nm (4.82 eV)
2nd	CIS 233.58 nm (5.31 eV) *f* = 0.5177 HOMO-5→LUMO+1: -0.15 HOMO-4→LUMO: 0.11 HOMO-4→LUMO+3: 0.11 HOMO-1→LUMO: 0.61 HOMO→LUMO+2: 0.20 CIS(D) 275.24 nm (4.50 eV)	CIS 235.14 nm (5.27 eV) *f* = 0.5325 HOMO-5→LUMO+1: -0.15 HOMO-4→LUMO: 0.11 HOMO-4→LUMO+3: 0.11 HOMO-1→LUMO: 0.61 HOMO→LUMO+2: 0.20 CIS(D) 275.36 nm (4.50 eV)
3rd	CIS 217.92 nm (5.69 eV) *f* = 0.3549 HOMO-5→LUMO+2: -0.13 HOMO-4→LUMO: 0.25 HOMO-2→LUMO: -0.11 HOMO-1→LUMO+3: 0.17 HOMO→LUMO+1: 0.56 CIS(D) 233.94 nm (5.30 eV)	CIS 218.92 nm (5.66 eV) *f* = 0.3192 HOMO-5→LUMO+2: -0.14 HOMO-4→LUMO: 0.26 HOMO-2→LUMO: 0.11 HOMO-1→LUMO+3: 0.17 HOMO→LUMO+1: 0.56 CIS(D) 236.55 nm (5.24 eV)

Table S14. Results of TDDFT with B3LYP/6-31G(d), SAC-CI/6-31G(d), CIS/3-21G, and CIS(D)/3-21G calculations of monomer of **1ar** with C2v symmetry-imposed structure optimized by B3LYP/6-31G(d).

Excited states	TDDFT with B3LYP/6-31G(d)	SAC-CI/6-31G(d)	CIS(D)/3-21G CIS/3-21G
1st	346.13 nm (3.58 eV) *f* = 0.7532 HOMO→LUMO: 0.70 Symmetry: B2	310.04 nm (4.00 eV) *f* = 0.1368 HOMO-1→LUMO: -0.79 Symmetry: A1	CIS(D) 278.76 nm (4.45 eV) CIS 237.89 nm (5.21 eV) *f* = 0.5917 Symmetry: A1
2nd	342.89 nm (3.62 eV) *f* = 0.1157 HOMO-1→LUMO: 0.65 HOMO→LUMO+1: -0.22 Symmetry: A1	287.86 nm (4.31 eV) *f* = 0.9781 HOMO→LUMO: 0.89 Symmetry: B2	CIS(D) 261.80 nm (4.74 eV) CIS 266.12 nm (4.66 eV) *f* = 1.0684 Symmetry: B2
3rd	295.90 nm (4.19 eV) *f* = 0.4069 HOMO-2→LUMO: 0.12 HOMO-1→LUMO: 0.22 HOMO→LUMO+1: 0.65 Symmetry: A1	256.67 nm (4.83 eV) *f* = 0.6277 HOMO→LUMO+1: -0.79 Symmetry: A1	CIS(D) 242.53 nm (5.11 eV) CIS 222.50 nm (5.57 eV) *f* = 0.3360 Symmetry: A1

* Although results of SAC-CI involve double excitations, only major contributions of single excitations are shown.

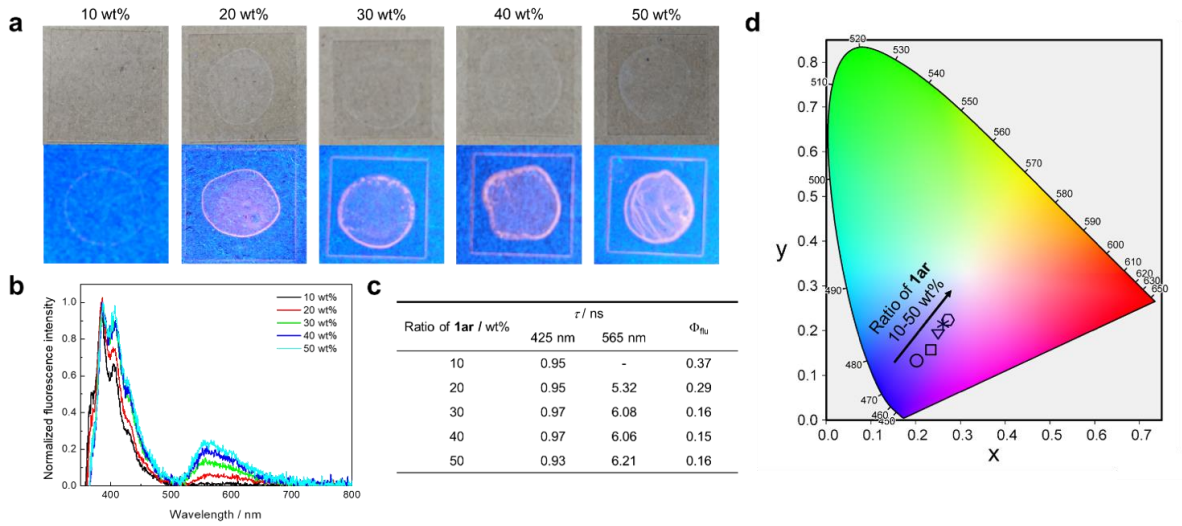

Fig. S21 (a) Photographs of fluorescence emission of **1ar**/PS composite films at various ratios of **1ar** (10-50 wt%) before (top) and under UV light (λ = 365 nm) irradiation (bottom). (b) Fluorescence spectrum of **1ar**/PS composite films (λ_{exc} = 340 nm). (c) Fluorescence lifetime (τ) and fluorescence quantum yield (Φ_{Flu}) of **1ar**/PS composite films. CIE 1931 coordinates of emission of **1ar**/PS composite films. The ratio of **1ar** was 10 (circle), 20 (square), 30 (triangle), 40 (asterisk), and 50 wt% (hexagon), respectively (λ_{exc} = 340 nm). These observations and measurements were performed at room temperature.

References

S1. H. E. Gottlieb, V. Kotlyar, A. Nudelman, *J. Org. Chem.* 1997, **62**, 7512–7515.

S2. J. V. Morris, M. A. Mahaney, J. R. Huber, *J. Phys. Chem.* 1976, **80**, 969–974.

S3. http://phonon-spectrum.com

S4. Gaussian 16, Revision C.01, M. J. Frisch, G. W. Trucks, H. B. Schlegel, G. E. Scuseria, M. A. Robb, J. R. Cheeseman, G. Scalmani, V. Barone, G. A. Petersson, H. Nakatsuji, X. Li, M. Caricato, A. V. Marenich, J. Bloino, B. G. Janesko, R. Gomperts, B. Mennucci, H. P. Hratchian, J. V. Ortiz, A. F. Izmaylov, J. L. Sonnenberg, D. Williams-Young, F. Ding, F. Lipparini, F. Egidi, J. Goings, B. Peng, A. Petrone, T. Henderson, D. Ranasinghe, V. G. Zakrzewski, J. Gao, N. Rega, G. Zheng, W. Liang, M. Hada, M. Ehara, K. Toyota, R. Fukuda, J. Hasegawa, M. Ishida, T. Nakajima, Y. Honda, O. Kitao, H. Nakai, T. Vreven, K. Throssell, J. A. Montgomery, Jr., J. E. Peralta, F. Ogliaro, M. J. Bearpark, J. J. Heyd, E. N. Brothers, K. N. Kudin, V. N. Staroverov, T. A. Keith, R. Kobayashi, J. Normand, K. Raghavachari, A. P. Rendell, J. C. Burant, S. S. Iyengar, J. Tomasi, M. Cossi, J. M. Millam, M. Klene, C. Adamo, R. Cammi, J. W. Ochterski, R. L. Martin, K. Morokuma, O. Farkas, J. B. Foresman, and D. J. Fox, Gaussian, Inc., Wallingford CT, 2016.

S5. P. Hohenberg, W. Kohn, *Phys. Rev.* 1964, **136**, B864–B871.

S6. W. Kohn, L. J. Sham, *Phys. Rev.* 1965, **140**, A1133-A1138.

S7. A. D. Becke, *Phys. Rev. A* 1988, **38**, 3098–3100.

S8. A. D. Becke, *J. Chem. Phys.* 1993, **98**, 5648–5652.

S9. C. Lee, W. Yang, R. G. Parr, *Phys. Rev. B* 1988, **37**, 785–789.

S10. S. Grimme, *J. Comp. Chem*. 2006, **27**, 1787–1799.

S11. http://www.jmol.org

S12. M. Head-Gordon, R. J. Rico, M. Oumi, T. J. Lee, *Chem. Phys. Lett.* 1994, **219**, 21–29.

S13. M. Head-Gordon, D. Maurice, M. Oumi, *Chem. Phys. Lett.* 1994, **246**, 114–21.

S14. R. E. Stratmann, G. E. Scuseria, M. J. Frisch, *J. Chem. Phys.* 1998, **109**, 8218–8224.

S15. R. Bauernschmitt, R. Ahlrichs, *Chem. Phys. Lett.* 1996, **256**, 454–464.

S16. M. E. Casida, C. Jamorski, K. C. Casida, D. R. Salahub, *J. Chem. Phys.* 1998, **108**, 4439–4449.

S17. N. J. Hestand, F. C. Spano, *Chem. Rev.* 2018, **118**, 7069–7163.

S18. F. Würthner, T. E. Kaiser, C. R. Saha-Möller, *Angew. Chem. Int. Ed.* 2011, **50**, 3376–3410.

S19. Z. He, W. Zhao, J. W.Y. Lam, Q. Peng, H. Ma, G. Liang, Z. Shuai, B. Z. Tang, *Nat. Commun.* 2017, **8**: 416.

S20. Q. Y. Yang, J. M. Lehn, *Angew. Chem. Int. Ed.* 2014, **53**, 4572–4577.

S21. X. H. Jin, C. Chen, C. X. Ren, L. X. Cai, J. Zhang, *Chem. Commun.* 2014, **50**, 15878–15881.

S22. H. Liu, X. Cheng, H. Zhang, Y. Wang, H. Zhang, S. Yamaguchi, *Chem. Commun.* 2017, **53**, 7832–7835.

S23. Z. Xie, C. Chen, S. Xu, J. Li, Y. Zhang, S. Liu, J. Xu, Z. Chi, *Angew. Chem. Int. Ed.* 2015, **54**, 7181–7184.

S24. S. Wang, G. Wang, X. Liang, D. Li, Z. Zhang, K. Guo, J. Li, Y. Miao, H. Wang, *Dyes Pigm.* 2022,

204, 110450.

S25. Y. C. Wei, Z. Zhang, Y. A. Chen, C. H. Wu, Z. Y. Liu, S. Y. Ho, J. C. Liu, J. A. Lin, P. T. Chou, *Commun. Chem.* 2019, **2**, Article number: 10.

S26. Y. Tsuchiya, K. Yamaguchi, Y. Miwa, S. Kutsumizu, M. Minoura, T. Murai, *Bull. Chem. Soc. Jpn.* 2020, **93**, 927–935.

S27. C. Zhou, S. Zhang, Y. Guo, H. Liu, T. Shan, X. Liang, B. Yang, Y. Ma, *Adv. Funct. Mater.* 2018, **28**, 1802407.

S28. Y. Wang, Q. Sun, L. Yue, J. Ma, S. Yuan, D, Liu, H. Zhang, S. Xue, W. Yang, *Adv. Opt. Mater.* 2021, **9**, 2101075.

S29. I. M. Resta, J. F. Miravet, M. Yamaji, F. Galindo, *J. Mater. Chem. C* 2020, **8**, 14348.

S30. N. N. Zhang, C. Sun, X. M. Jiang, X. S. Xing, Y. Yan, L. Z. Cai, M. S. Wang, G. C. Guo, *Chem. Commun.* 2017, **53**, 9269–9272

S31.